NUMERICAL SIMULATIONS OF RUBBER BEARING TESTS AND SHAKING TABLE TESTS

K. HIRATA, A. MATSUDA, S. YABANA
Central Research Institute of Electric Power Industry, Japan

Abstract

Test data concerning rubber bearing tests and shaking table tests of base-isolated model conducted by CRIEPI are provided to the participants of Coordinated Research Program (CRP) on "Intercomparison of Analysis Methods for predicting the behaviour of Seismically Isolated Nuclear Structure", which is organized by International Atomic Energy Agency (IAEA), for the comparison study of numerical simulation of base-isolated structure. In this paper outlines of the test data provided and the numerical simulations of bearing tests and shaking table tests are described. Using computer code ABAQUS, numerical simulations of rubber bearing tests are conducted for NRBs, LRBs (data provided by CRIEPI) and for HDRs (data provided by ENEA/ENEL and KAERI). Several strain energy functions are specified according to the rubber material test corresponding to each rubber bearing. As for lead plug material in LRB, mechanical characteristics are reevaluated and are made use of. Simulation results for these rubber bearings show satisfactory agreement with the test results. Shaking table test conducted by CRIEPI is of a base isolated rigid mass supported by LRB. Acceleration time histories, displacement time histories of the isolators as well as cyclic loading test data of the LRB used for the shaking table test are provided to the participants of the CRP. Simulations of shaking table tests are conducted for this rigid mass, and also for the steel frame model which is conducted by ENEL/ENEA. In the simulation of the rigid mass model test, where LRBs are used, isolators are modeled either by bilinear model or polylinear model. In both cases of modeling of isolators, simulation results show good agreement with the test results. In the case of the steel frame model, where HDRs are used as isolators, bilinear model and polylinear model are also used for modeling isolators. The response of the model is simulated comparatively well in the low frequency range of the floor response, however, in the high frequency range discrepancies from the test result becomes larger, implying the requirement of more detailed or proper modeling of the rubber bearing and the steel frame.

1. INTRODUCTION

In Japan, the demonstration test for FBR base isolation system has been carried out in the past decade by several organizations In particular, CRIEPI (Central Research Institute of Electric Power Industry) has played a leading role in this project and conducted various isolator tests, shaking table tests, and the design guidelines for FBR base isolation system are prepared by CRIEPI. CRIEPI, as a participant of Coordinated Research Program (CRP) on Intercomparison of Analysis Methods for Seismically Isolated Nuclear Structure organized by International Atomic Energy Agency (IAEA), provided rubber bearing test data and shaking table test data to the participants of the CRP. The CRP started in 1996 and continued until 1999. In this CRP the test data have been used for the intercomparison of the simulation, and the results of the numerical simulations that CRP participants have conducted are reported and the related information have been exchanged at the RCM (Research Coordination Meeting) of this CRP.

2. RUBBER BEARING TESTS CONDUCTED IN CRIEPI

2.1. Testing facilities

Static two-dimensional loading test machine designed and manufactured especially for testing isolation element was used (Fig. 1). The machine is composed of two actuators giving axial and shear force to test specimens, and the actuators are controlled under load control mode and/or displacement control mode. Maximum available load of each actuator is 600 tons. Maximum shear displacement available is ± 600 mm (bi-directional mode) or 1200 mm (unidirectional mode), and maximum axial displacement available is ± 350 mm (bi-directional mode) or 700 mm (unidirectional mode). By using this machine full-scale rubber bearing tests and scale model tests have been conducted. Even using this test machine it is impossible to give rubber bearings large deformation to cause rupture, and scale-models of rubber bearing are used for the break test.

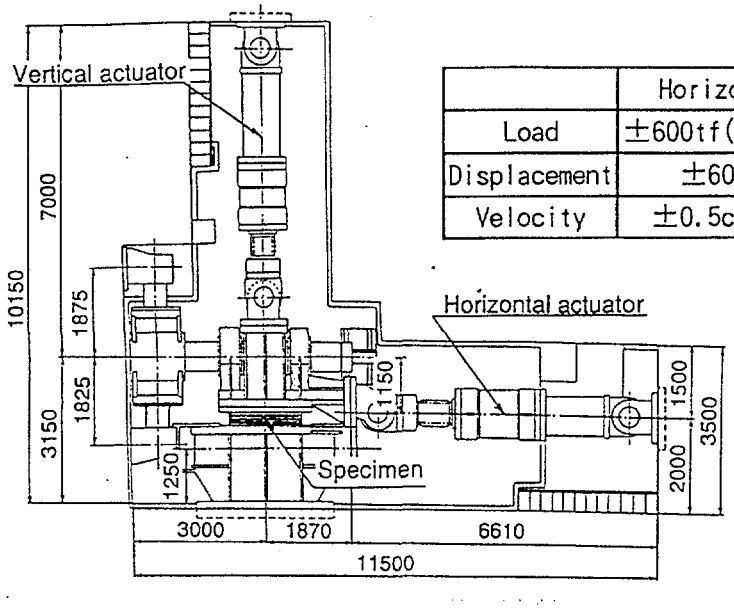

	Horizontal	Vertical
Load	±600tf(5880kN)	±600tf(5880kN)
Displacement	±600mm	±350mm
Velocity	±0.5cm/sec	±0.5cm/sec

Fig. 1 Schematic view of static test machine

2.2. Specifications and geometrical data of NRB

Full-scale NRB presumed to be used for the FBR building is 1600 mm in diameter and its design vertical load is 500–1000 tons. Test data for the scale models of NRB (Scale: 1/1.58 and 1/3.168) [8][12][13] are used for the comparative study between the experiment and the numerical simulation.

Specifications and geometrical data of the scale models of the NRB are as follows.

(1) 200 ton NRB
[Specifications]
- Design vertical load: 200 tons (1/1.58 scale model of prototype 500 tons bearing)

- Design vertical stress: 25 kgf/cm^2
- Horizontal frequency fh of Prototype: 0.5 Hz (Th = 2 sec)
- Vertical frequency fv of Prototype: > 20 Hz
- Shear modulus G 6 kgf/cm^2

[Geometrical data]
- Thickness of rubber sheet: 5.7 mm
- Number of rubber layers: 25
- Thickness of rubber layers: 142.5 mm (5.7 mm × 25)
- Thickness of steel plate: 3.1 mm
- Number of steel plates: 24
- Diameter of rubber D: 1012 mm
- Inner diameter of rubber D_i: 126 mm
- Primary shape factor Sc1: 38.9

(2) 50 ton NRB
[Specifications]
- Design vertical load: 50 tons (1/3.168 scale model of prototype 500 tons bearing)
- Design vertical stress: 25 kgf/cm^2
- Horizontal frequency fh of Prototype: 0.5 Hz (Th = 2sec)
- Vertical frequency fv of Prototype: > 20 Hz
- Shear modulus G 6 kgf/cm^2

[Geometrical data]
- Thickness of rubber sheet: 2.8 mm
- Number of rubber layers: 25
- Total thickness of rubber layers: 70 mm (2.8 mm × 25)
- Thickness of steel plate: 1.6 mm
- Number of steel plates: 24
- Diameter of rubber D: 506 mm
- Inner diameter of rubber D_i 63 mm
- Primary shape factor Sc1: 38.9

2.3. Specifications and geometrical data of LRB with thin lead plug

Full-scale LRB presumed to be used for the FBR building is 1600 mm in diameter and its design vertical load is 500–1000 tons. Test data on the scale model of LRB (Scale: 1/1.83 and 1/3.16) [8][12][13] are used for the comparative study between the experiment and the numerical simulation.

Specifications and geometrical data of the scale models of the LRB are as follows.

(1) 150 ton LRB
[Specifications]

- Design vertical load: 150 tons (1/1.83 scale model of prototype 500 tons bearing)
- Design vertical stress: 25 kgf/cm^2
- Horizontal frequency fh of Prototype: 0.5 Hz (Th = 2 sec)
- Vertical frequency fv of Prototype: > 20 Hz
- Shear modulus G 6 kgf/cm^2

[Geometrical data]
- Thickness of rubber sheet: 4.9 mm
- Number of rubber layers: 25
- Total thickness of rubber layers: 122.5 mm (4.9 mm × 25)
- Thickness of steel plate: 3.1 mm
- Number of steel plates: 24
- Diameter of rubber D: 876 mm
- Inner diameter of rubber D_i: 98 mm
- Diameter of lead plug 98 mm
- Height of lead plug > 196.9 mm
- Primary shape factor Sc1: 39.4

(2) 50 ton LRB
[Specifications]
- Design vertical load: 50 tons (1/3.16 scale model of prototype 500 tons bearing)
- Design vertical stress: 25 kgf/cm^2
- Horizontal frequency fh of Prototype: 0.5 Hz (Th = 2sec)
- Vertical frequency fv of Prototype: > 20 Hz
- Shear modulus G 6 kgf/cm^2

[Geometrical data]
- Thickness of rubber sheet: 2.8 mm
- Number of rubber layers: 25
- Total thickness of rubber layers: 70 mm (2.8 mm × 25)
- Thickness of steel plate: 1.6 mm
- Number of steel plates: 24
- Diameter of rubber D: 506 mm
- Inner diameter of rubber D_i: 57 mm
- Diameter of lead plug 57 mm
- Height of lead plug > 108.4 mm
- Primary shape factor Sc1: 39.4

2.4. Specifications and geometrical data of LRB with thick lead plug

LRB described in the subsection 2.3 has comparatively thin lead plug. Diameter ratio of the lead plug to the rubber is 1:8.9 (= 98 mm: 876 mm) and there arises a question that the accuracy of the simulation on lead plug part may not influence the simulated

force-displacement relationship of LRB as a whole. For this reason test data of LRB with thick lead plug was provided by JAERI/CRIEPI, in which the diameter ratio of lead plug to rubber is 1:4, for additional case of numerical simulation.

Specifications and geometrical data of the scale models of these LRB are as follows.

(1) ϕ 500-LRB

[Specifications]

- Design vertical load:	181.25 tons (500/1200 scale model of prototype 1044 tons bearing)
- Design vertical stress:	100 kgf/cm^2
- Horizontal frequency fh of Prototype:	0.25 Hz (Th = 4 sec)
- Vertical frequency fv of Prototype:	10 Hz

[Geometrical data]

- Thickness of rubber sheet:	3.6 mm
- Number of rubber layers:	23
- Total thickness of rubber layers:	82.8 mm (3.6 mm × 23)
- Thickness of steel plate:	2.5 mm
- Number of steel plates:	22
- Diameter of rubber D:	500 mm
- Inner diameter of rubber D_i:	125 mm
- Diameter of lead plug	125 mm
- Height of lead plug	152.8mm
- Primary shape factor Sc1:	32.6

(2) ϕ 280-LRB

[Specifications]

- Design vertical load:	56.84 tons (280/1200 scale model of prototype 1044 tons bearing)
- Design vertical stress:	100 kgf/cm^2
- Horizontal frequency fh of Prototype:	0.25 Hz (Th = 4 sec)
- Vertical frequency fv of Prototype:	10 Hz

[Geometrical data]

- Thickness of rubber sheet:	2.0 mm
- Number of rubber layers:	23
- Total thickness of rubber layers:	46 mm (2.0 mm × 23)
- Thickness of steel plate:	2.5 mm
- Number of steel plates:	22
- Diameter of rubber D:	280 mm
- Inner diameter of rubber D_i:	70 mm
- Diameter of lead plug	70 mm
- Height of lead plug	93.6 mm
- Primary shape factor Sc1:	32.6

In this case, NRB with the same rubber material and geometrical shape of laminated rubber part as the above-described LRB was tested to investigate the effect of the lead plug. As is shown in the subsequent section this result was used to "extract" mechanical characteristics of lead plug from the test result of LRB.

2.5. Test methods and results

Three kinds of rubber bearing tests, i.e. horizontal cyclic loading test, vertical cyclic loading test and failure test were conducted [12][13].

Horizontal cyclic loading tests were conducted to evaluate horizontal stiffness and damping of the rubber bearing. These tests are performed giving shear loading of low frequency (under 0.01 Hz) with axial loading. Four cycles of sinusoidal shear deformation are applied to rubber bearings under constant vertical load. For the evaluation of the stiffness and the damping of the rubber bearing, loading test data of the third cycle is usually used. Amplitude of shear deformation is varied from ± 25 to ± 400% of shear strain of the rubber.

Vertical cyclic loading tests were conducted to evaluate vertical stiffness and damping of the rubber bearing. These tests are conducted giving vertical loading of low frequency in the same way as the horizontal cyclic loading test. In this test also four cycles of sinusoidal vertical loading is applied after giving initial static vertical load and constant shear strain (offset shear strain). Amplitude of the applied sinusoidal vertical loading is up to 200% of the design vertical load.

Failure tests are conducted to evaluate ultimate capacity of the rubber bearings and their mechanical characteristics in the ultimate state. Test data provided to the participants of the CRP are concerning shear failure tests in which under constant vertical load shear deformation is given to the rubber bearing until failure occurs. In the shear failure tests, four cycles of static sinusoidal shear load is first applied up to 400% of shear strain under design vertical loading, then horizontal deformation is given monotonically until the failure of rubber bearing occurs.

3. SIMILATION OF THE BEARING TESTS

3.1. Material properties

3.1.1. Properties of natural rubber material

In the simulation of shear loading tests of NRB and LRB which were conducted in CRIEPI, following strain energy functions for deviatoric components proposed by Seki [16] are used.

$$W = \sum_{i=1}^{2}[a_i(I_i-3)+\frac{b_i}{2}(I_i-3)^2+\frac{c_i}{3}(I_i-3)^3+\frac{d_i}{e_i}\exp(e_i(I_i-3))] \quad (1)$$

where W is the strain energy function, I_1 and I_2 are invariants expressed by stretches principal $\lambda_1, \lambda_2, \lambda_3$ as,

$$I_1 = \lambda_1^2 + \lambda_2^2 + \lambda_3^2 \quad I_2 = \lambda_1^2\lambda_2^2 + \lambda_2^2\lambda_3^2 + \lambda_3^2\lambda_1^2 \qquad (2)$$

and coefficients a_i, b_i, d_i, c_i and e_i are obtained from biaxial tensile test of the rubber sheet as [16],

$a_1 = 2.09$, $b_1 = 1.35\times 10^{-1}$, $c_1 = 2.4\times 10^{-3}$, $d_1 = 1.75$, $e_1 = -2.12$, $a_2 = 0.138$, $b_2 = -1.64\times 10^{-2}$, $c_2 = 6.44\times 10^{-4}$, $d_2 = -0.7$, $e_2 = -6.44$ (unit: kgf/cm^2)

For volumetric component, following strain energy function is used.

$$U = \sum_{i=1}^{4} \frac{1}{D_i}(J^{el} - 1)^{2i} \qquad (3)$$

where J^{el} is the elastic volume ratio and the coefficients D_i are obtained from the volumetric compression test as [11],

$D_1 = 3.366\times 10^{-4}$, $D_2 = 3.297\times 10^{-8}$, $D_3 = -8.709\times 10^{-12}$, $D_4 = 7.295\times 10^{-15}$ (unit: kgf/cm^2)

3.1.2. Properties of high damping rubber material (1)

In the simulation of shear loading test of HDR conducted in Italy following strain energy function of polynomial form [6] is used, and the coefficients were determined from the material test data provided from Italy. The function is given as,

$$U = \sum_{i+j=1}^{2} C_{ij}(\bar{I}_1 - 1)^i(\bar{I}_2 - 1)^j + \sum_{i=1}^{2} \frac{1}{D_i}(J^{el} - 1)^{2i} \qquad (4)$$

where $\bar{I}_1$ *and* $\bar{I}_2$ are the first and the second deviatoric strain invariants. Coefficients C_{ij} and D_i are determined from the tensile test data of the rubber sheet and the volumetric test data of the rubber, which were provided from Italy.

3.1.3. Properties of high damping rubber material (2)

In the simulation of the shear loading test of HDR conducted in Korea strain energy function of polynomial form expressed by Eq. (4) and Ogden's formulation given below are used. In both formulations, coefficients were determined from the material test data provided from Korea.

$$U = \sum_{i=1}^{6} C_{ij} \frac{2\mu_i}{\alpha_i^2}(\bar{\lambda}_1^{\alpha i} + \bar{\lambda}_2^{\alpha i} + \bar{\lambda}_3^{\alpha i} - 3) + \sum_{i=1}^{6} \frac{1}{D_i}(J^{el} - 1)^{2i} \qquad (5)$$

3.1.4. Properties of lead

Mechanical properties of the lead used in LRB were determined by two ways. In the first way, material properties was determined from the test results of uniaxial tensile test of the lead specimen as [7],

- Young's modulus E = 1750 kgf/mm^2
- Poisson's ratio $\nu = 0.44$
- Yield stress = 0.2 kgf /mm^2

After yielding, stress-strain relationship of the lead used is expressed as [7]

$$\sigma_t = 4.0(1+0.096\log_{10}\varepsilon_t)\varepsilon_t^{0.31} \quad (6)$$

where σ_t and ε_t are the tensile true stress and true strain of lead respectively, and ε_t is the true strain rate of the lead. And isotropic hardening rule is applied.

In the second way, the test results of LRB with thick lead plug and NRB are used, where force-displacement relationship of the NRB is subtracted from that of the LRB and the stress-strain relationship of the lead plug is evaluated considering that the lead plug is subjected to pure shear deformation [5] (Fig. 2). In this case, the lead is modeled as an elasto-plastic material with the following characteristics;

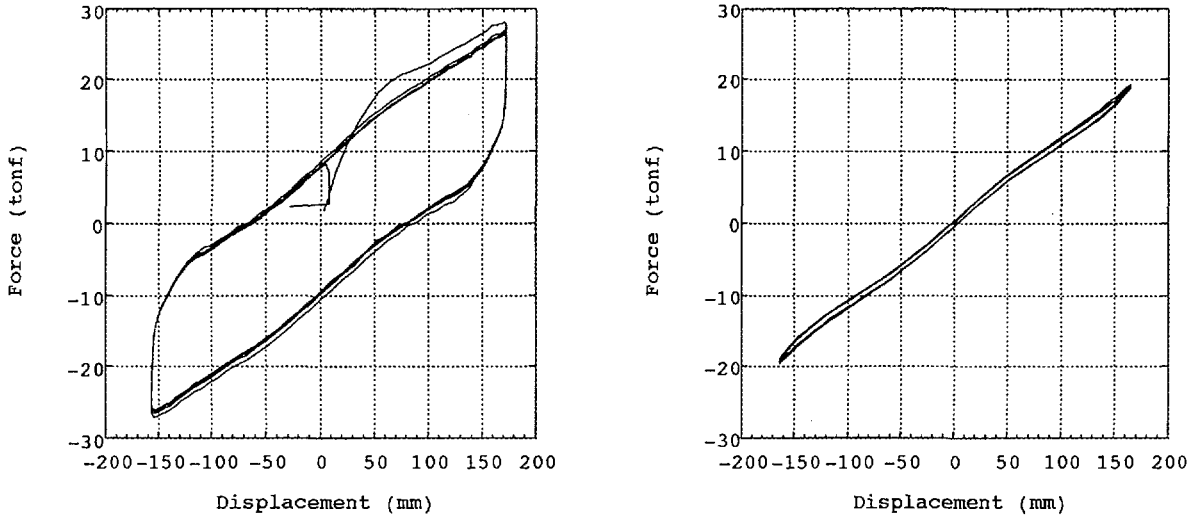

(a) Hysteresis loop of LRB

(b) Hysteresis loop of NRB

Fig. 2 Hysteresis loop of lead plug extracted from LRB and NRB tests

- Young's modulus $E_0 = 1166.6$ kgf/cm^2
- Poisson's ratio $\nu = 0.44$

and the stress-strain (logarithmic strain) relationship is given as multi-linear expression (Fig. 3).

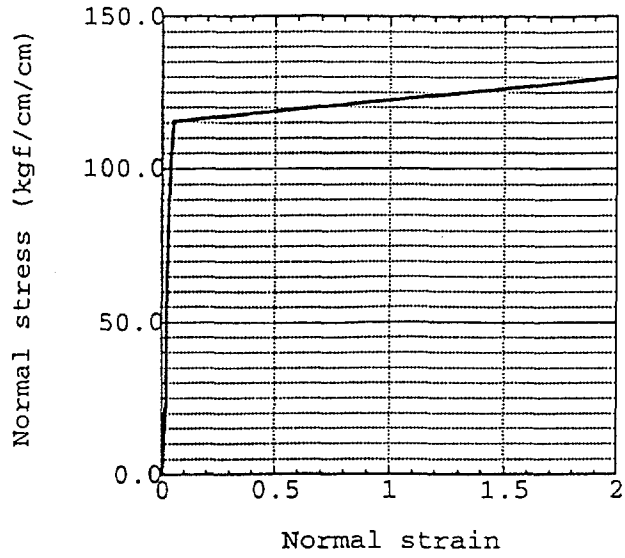

Fig. 3 Stress-strain relationship of lead

3.1.5. Properties of steel

Material properties of the steel for the steel shim plate are as follows.

- Young's modulus $E = 1.97 \times 10^4$ kgf/mm^2
- Poisson's ratio = 0.271
- Yield stress $c_y = 25.5$ kgf/mm^2

As for hardening rule, isotropic hardening is assumed. However, in the simulation of the rubber bearings yielding of the steel shim plate did not to occur.

3.2. Computer code and computational conditions

Bearing test data on NRB and LRB provided by CRIEPI and test data on HDR provided by ENEA were used for the comparison between the experiment and the numerical simulation. Numerical simulation was conducted using computer code ABAQUS [6]. For the rubber and the lead plug 8-node linear brick, hybrid, constant pressure element C3D8H (ABAQUS/Standard User's Manual, 1996)is used, and C3D8I element is used for the steel shim plate. In the simulation of LRB continuity between the lead plug and other part of the

bearing is assumed (i.e. no sliding is allowed). Half section model of the rubber bearings was used and divided into 6 elements in radial direction and 8 elements in circumferential direction. Lead plug of LRB is divided into 2 elements in radial direction and 8 elements in circumferential direction. Each rubber layer and steel shim plate is divided respectively into 3 and 2 layers (Fig. 4).

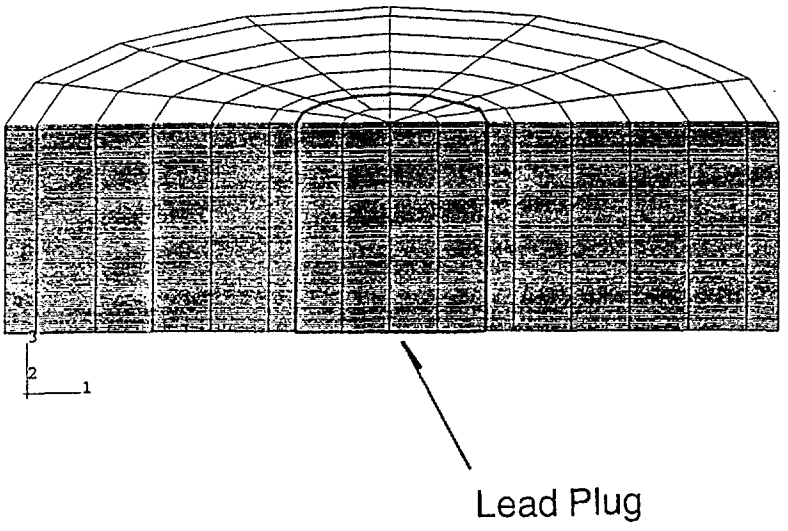

Fig. 4 Finite element mesh of HDR with thick lead plug

3.3. Results of numerical simulation

3.3.1. Simulation of NRB test

Numerical simulations were conducted for the bearings of different scale with similar geometrical shape, i.e. "200 ton NRB" and "50 ton NRB". The bearing tests are; shear loading test under design compressive load and compressive loading test with 0% shear strain of rubber bearing. Comparisons of numerical simulations and the test results are shown in Figs. 5 through 8. In the case of the shear deformation tests simulated results show good agreement with the initial loading curve of the test results up to the shear deformation of about 600 mm for 200 ton NRB and 260 mm for 50 ton NRB (or 400% of shear strain).

As for the compressive loading test, simulated results show good agreement with the experimental results.

3.3.2. Simulation of LRB test

Numerical simulations were conducted for the tests of two types of LRB conducted in CRIEPI. One type is the LRB with slender lead plug, "150 ton LRB" and "50 ton LRB" with similar geometrical shape. Another type is the LRB with thick lead plug. The bearing tests are; shear loading test under design compressive load and compressive loading test with 0% shear strain of rubber bearing (for LRB with slender lead plug).

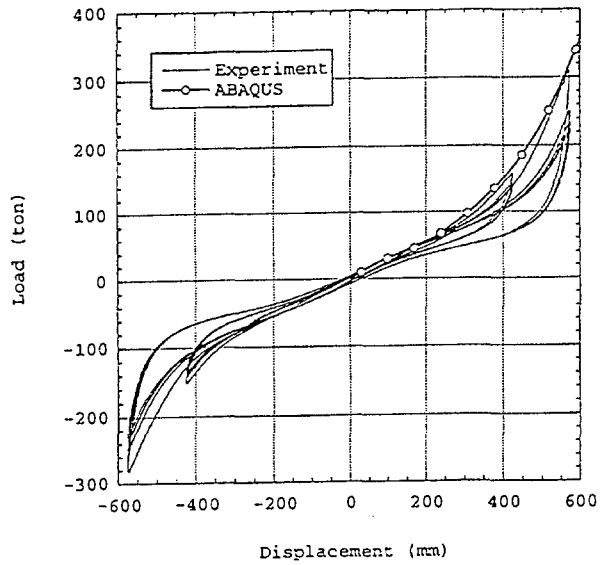

Fig. 5 Experiment and simulation of horizontal loading ('200 ton NRB' under vertical load of 200tons)

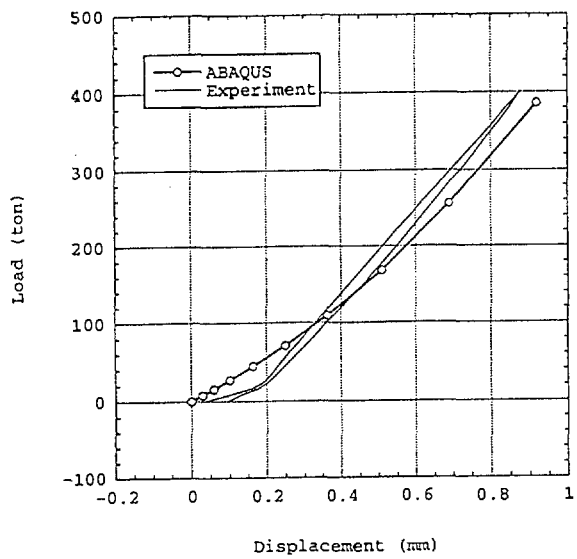

Fig. 6 Experiment and simulation of vertical loading ('200 ton NRB' with 0% offset shear strain)

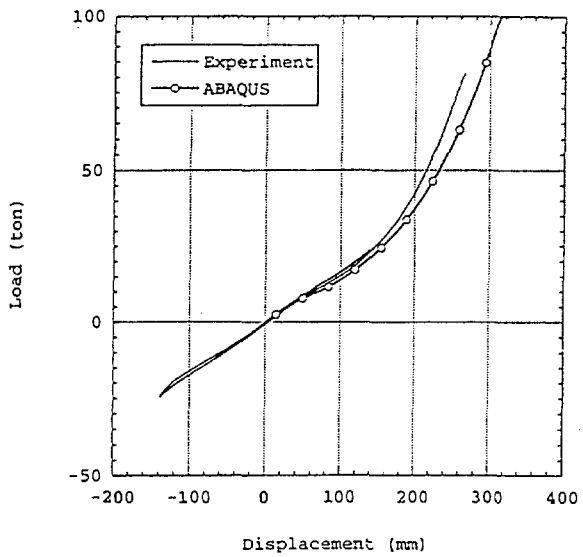

Fig. 7 Experiment and simulation of horizontal loading ('50 ton NRB' under vertical load of 50 tons)

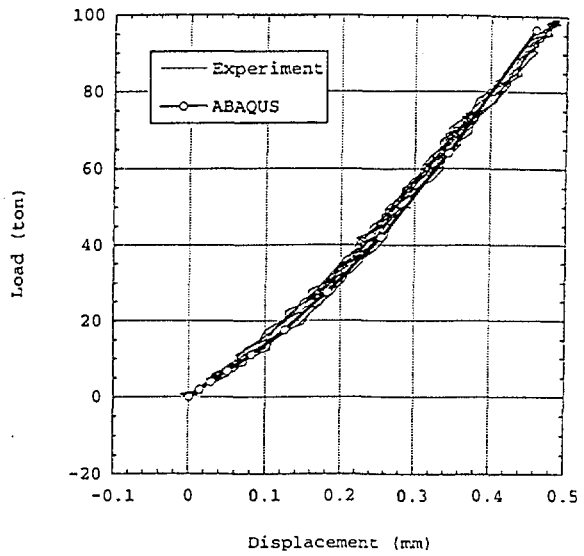

Fig. 8 Experiment and simulation of vertical loading ('50 ton NRB' with 0% offset shear strain)

At first, numerical simulation was conducted using mechanical characteristics of lead given by Eq. (6). For the LRB with thin lead plug (diameter ratio of lead to rubber = 1:8.9), numerical simulations show good agreement with test results for both shear loading and vertical loading tests (Figs. 9 through 12). However, for the LRB with thick lead plug numerical simulation did not agree well with the test result. Using mechanical characteristics of the lead shown in Fig. 3, numerical simulation was conducted, proving that the numerical simulation showed good agreement with the test results (Fig. 13). In Fig. 13 "old" and "new"

mean simulation with lead properties given by Eq. (6) and Fig. 3 respectively. Using this lead characteristic, simulation of LRB with slender lead plug was also conducted. The result shows that this mechanical characteristic is also valid for the LRB of different geometrical shape (Fig. 14; "old" and "new" are used in the same sense as in Fig. 13) and can be regarded as a general one for the lead plug under pure shear deformation.

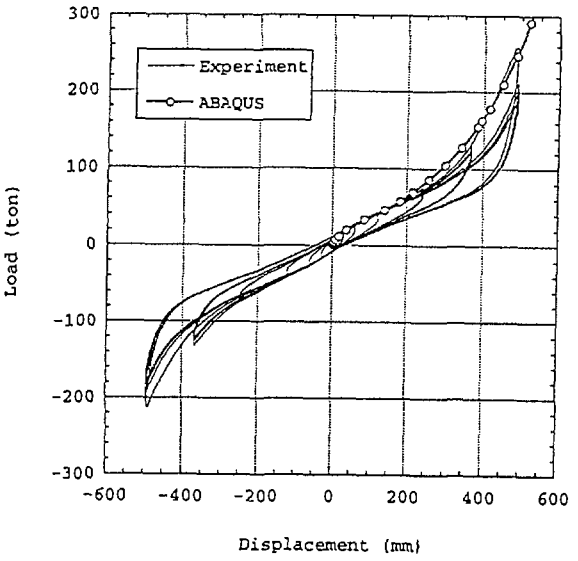

Fig. 9 Experiment and simulation of horizontal loading ('150 ton LRB' under vertical load of 150 tons)

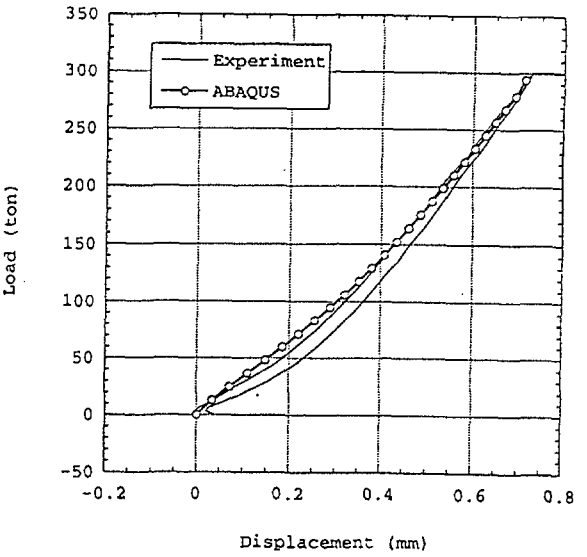

Fig. 10 Experiment and simulation of vertical loading ('150 ton LRB' with 0% offset shear strain)

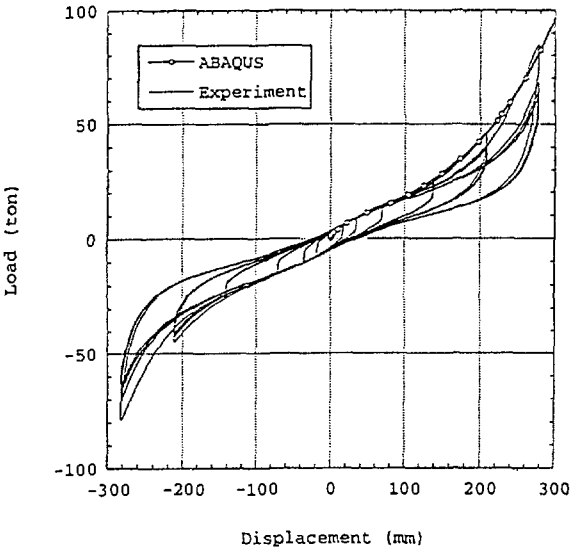

Fig. 11 Experiment and simulation of horizontal loading ('50 ton LRB' under vertical load of 50tons)

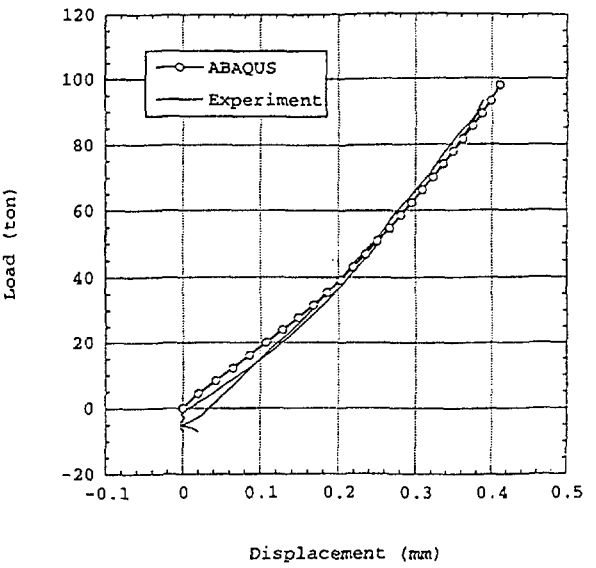

Fig. 12 Experiment and simulation of vertical loading ('50 ton LRB' with 0% offset shear strain)

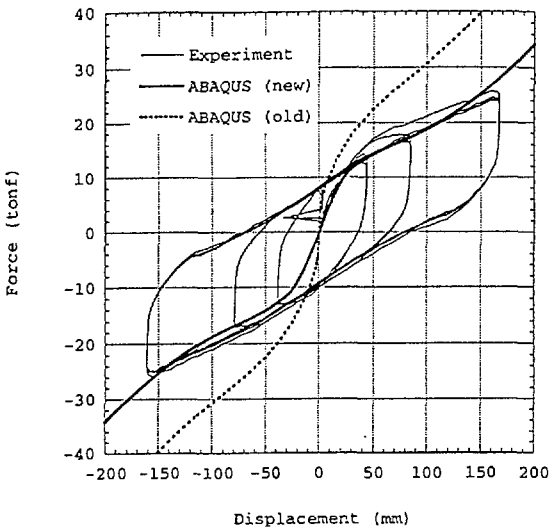

Fig. 13 Force - displacement relationship of LRB with thick lead plug (Test and Simulation)

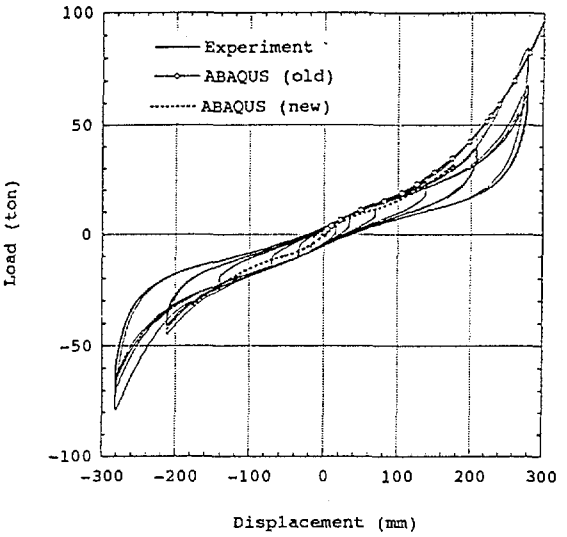

Fig. 14 Experiment and simulation of horizontal loading ('50 ton LRB' under vertical load of 50tons)

3.3.3. Simulation of HDR test

Numerical simulations were conducted for the bearing test conducted in Italy and Korea. Figs. 15 and 16 show the results of the simulation for the shear loading test of HDR conducted by ENEL/ENEA [1][2]. In these cases simulated results agree well with the test results up to about 50 mm of shear deformation (or about 160% of shear strain of rubber or higher). Fig. 17 shows the result of the simulation for the compressive loading test of HDR. In this case both simulated and test results show good agreement, particularly, nonlinear relationship between force and displacement is simulated satisfactorily.

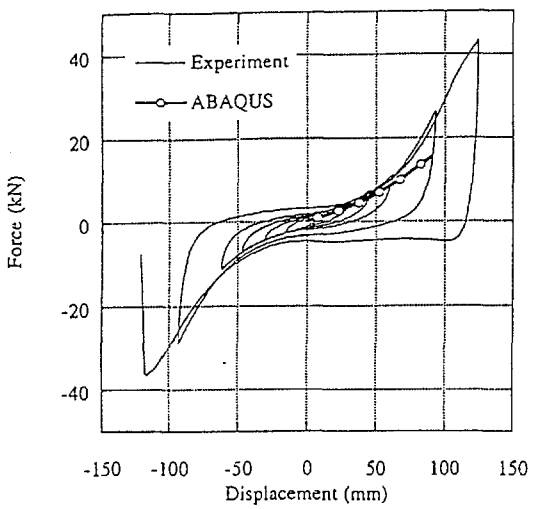

Fig. 15 Experiment and simulation of shear loading (HDR data from Italy, Compressive load: 50kN)

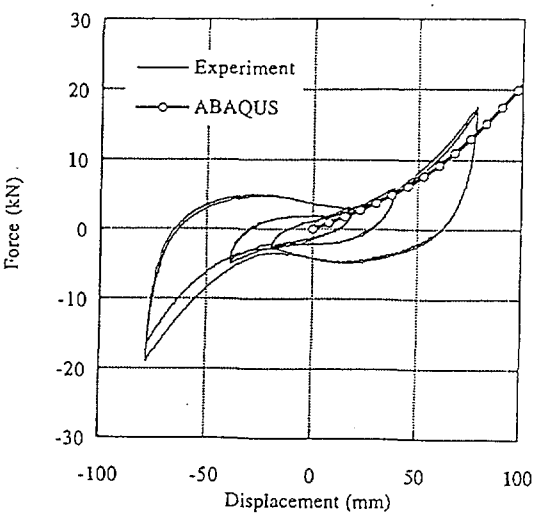

Fig. 16 Experiment and simulation of shear loading (HDR data from Italy, Compressive load: 100kN)

Figs. 18 and 19 show results of shear loading test of HDR provided by KAERI, results of cyclic loading test and failure test under monotonical loading [18]. Numerical simulations were conducted using two types of strain energy function; polynomial formulation given by Eq. (4) and Ogden's formulation given by Eq. (5). For the cyclic loading tests, numerical simulation using strain energy function of polynomial formulation seems to give better agreement with the test. However, for the failure test, where displacement is larger than the cyclic loading test, simulation using Ogden's formulation gives better results.

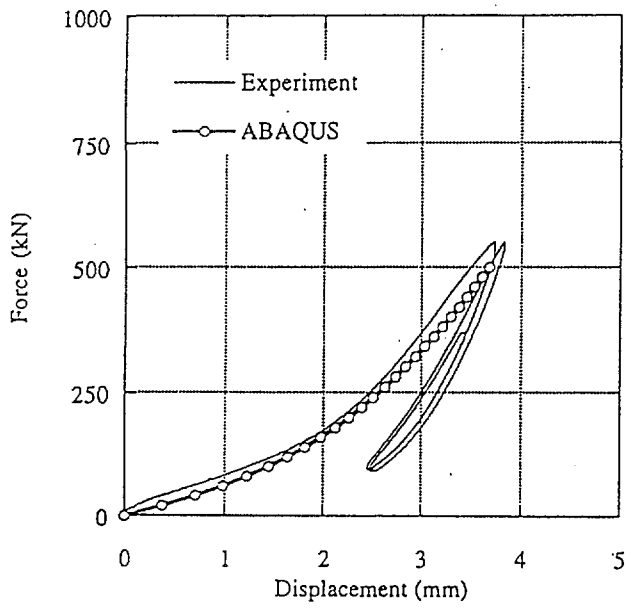

Fig. 17 Experiment and simulation of vertical loading
(HDR data from Italy, Offset shear strain 0%)

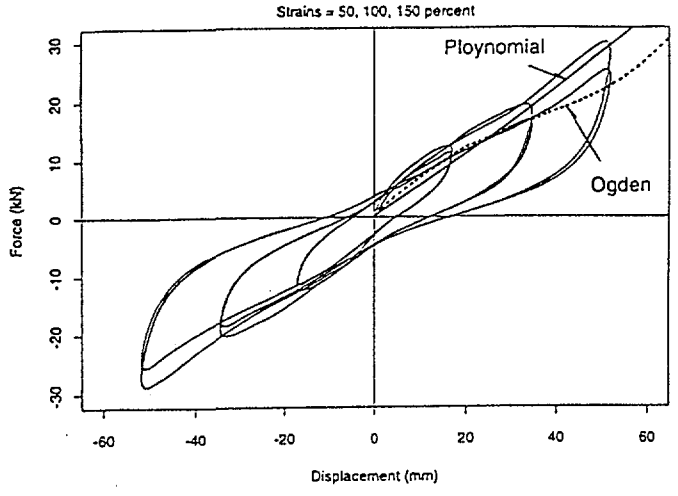

Fig. 18 Experiment and simulation of shear loading
(HDR data from Korea)

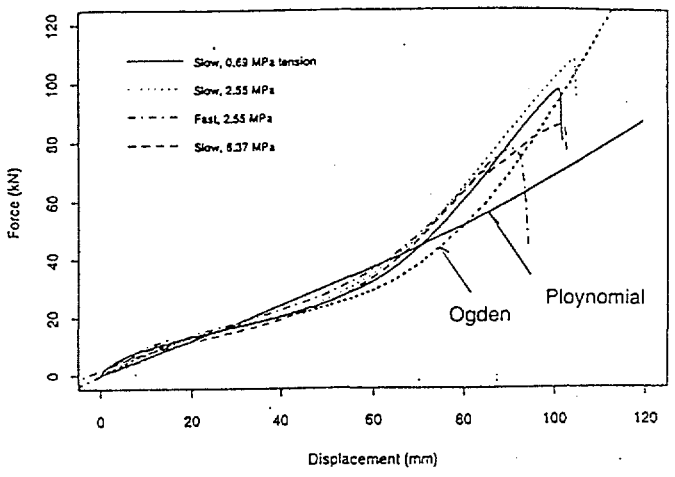

Fig. 19 Experiment and simulation of failure test
(HDR data from Korea)

4. SHAKING TABLE TESTS CONDUCTED BY CRIEPI

4.1. Outline of the test

Shaking table test of a scale model of rigid isolated structure was conducted by CRIEPI [9][14]. The main purpose of the test is to investigate dynamic behavior of isolated structure and the rubber bearings under extremely strong earthquake. Increasing the input acceleration level, response characteristics of the base-isolated model up to the vicinity of the ultimate state of the rubber bearings was investigated. The model is a rigid mass of 17.8 ton weight supported by 8 LRBs (Fig. 20). Similitude applied to the shaking table test is determined considering following points.

- Stress of the model bearings be equal to that of the prototype
- Amplitude of input acceleration to the model structure be equal to that of the prototype
- Geometrical shape of the model bearing be similar to that of the prototype with the scale of 1/15.

LRBs used in the test are geometrically 1/15 reduced scale of prototype bearing supporting vertical load of 2.25 tons each. Rubber bearing tests of the bearings were performed before the shaking table test and the test results are shown in Fig. 21.

In Japan two levels of design earthquake motion S1 and S2 are used in the seismic design of nuclear power plant. In the shaking table test, input earthquake motion S1 consistent with the tentative design spectrum proposed for the base-isolated nuclear power plant was used basically. In this case amplitude of the input earthquake motion S2 is 1.5 times as large as that of S1 (i.e. S2 = 1.5 × S1). For the purpose of the comparison between the test and the simulation, test results for the input motion of design earthquake motion S2 (=1.5×S1) and the those for the input motion three times as large as the design earthquake motion (3×S2) are provided to the participants of the CRP.

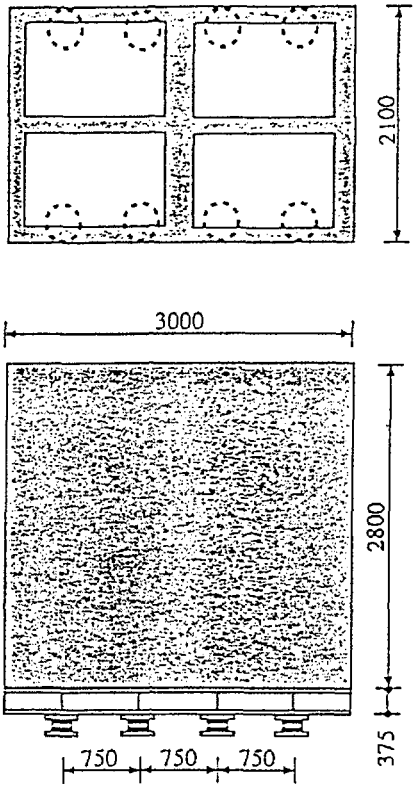

Fig. 20 Schematic view of base-isolated rigid mass

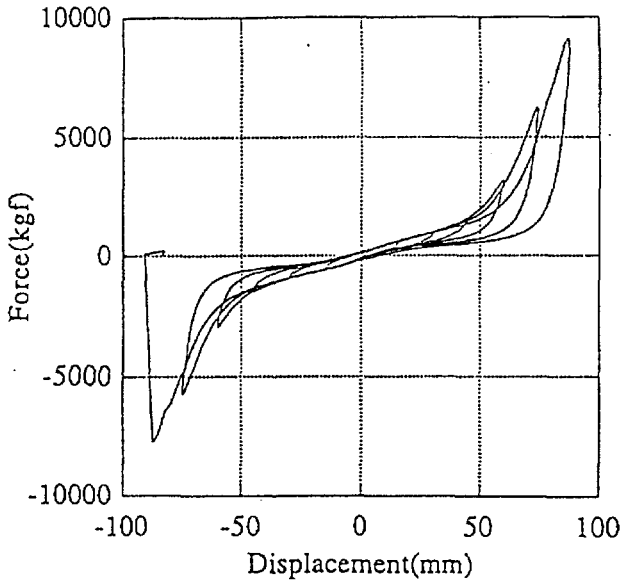

Fig. 21 Shear loading test of LRB used for base-isolated rigid mass

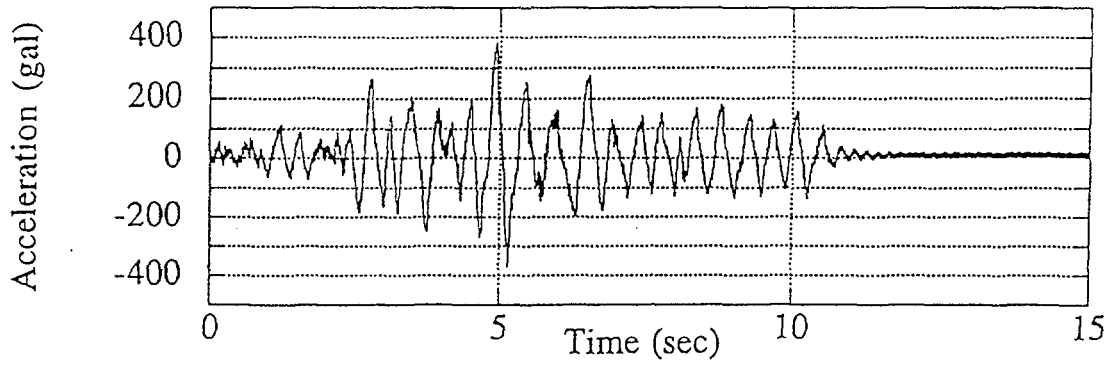

Fig. 22 Response acceleration of rigid mass (top)

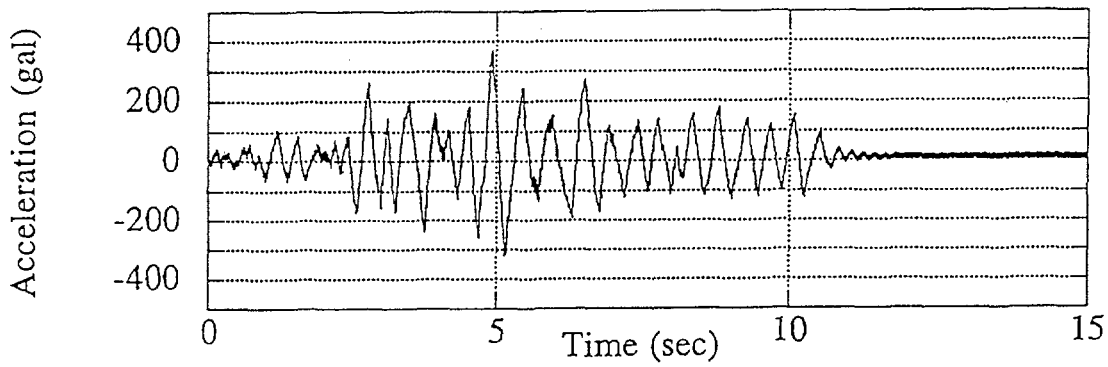

Fig. 23 Response acceleration of rigid mass (base)

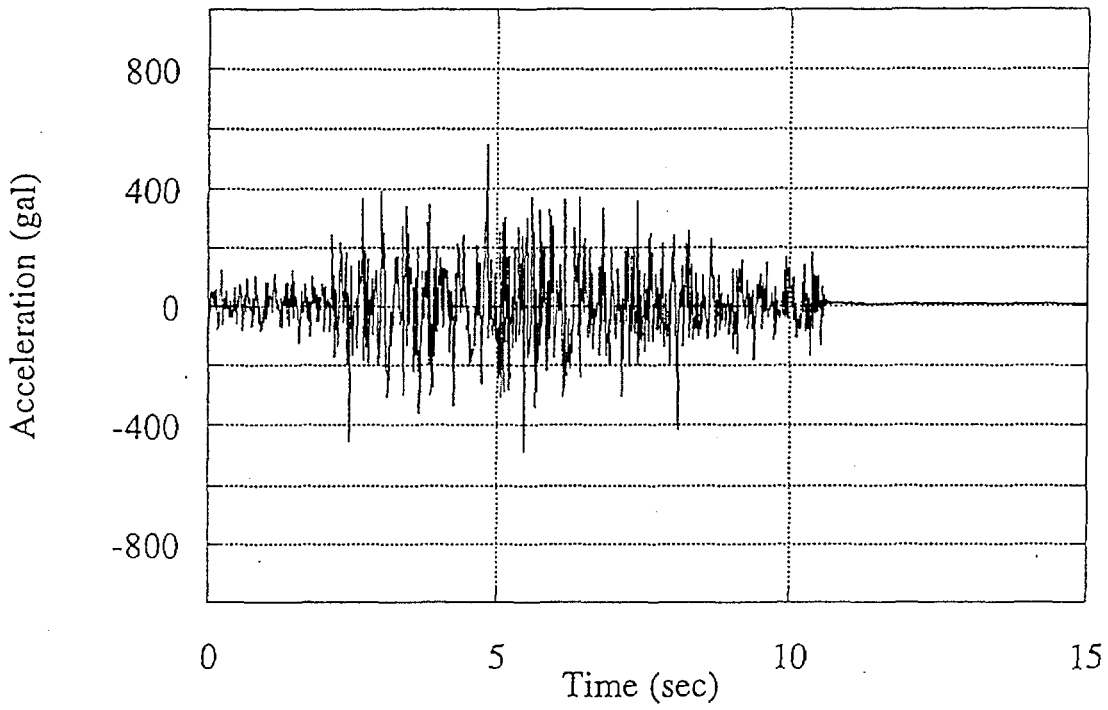

Fig. 24 Input acceleration (1.5S1)

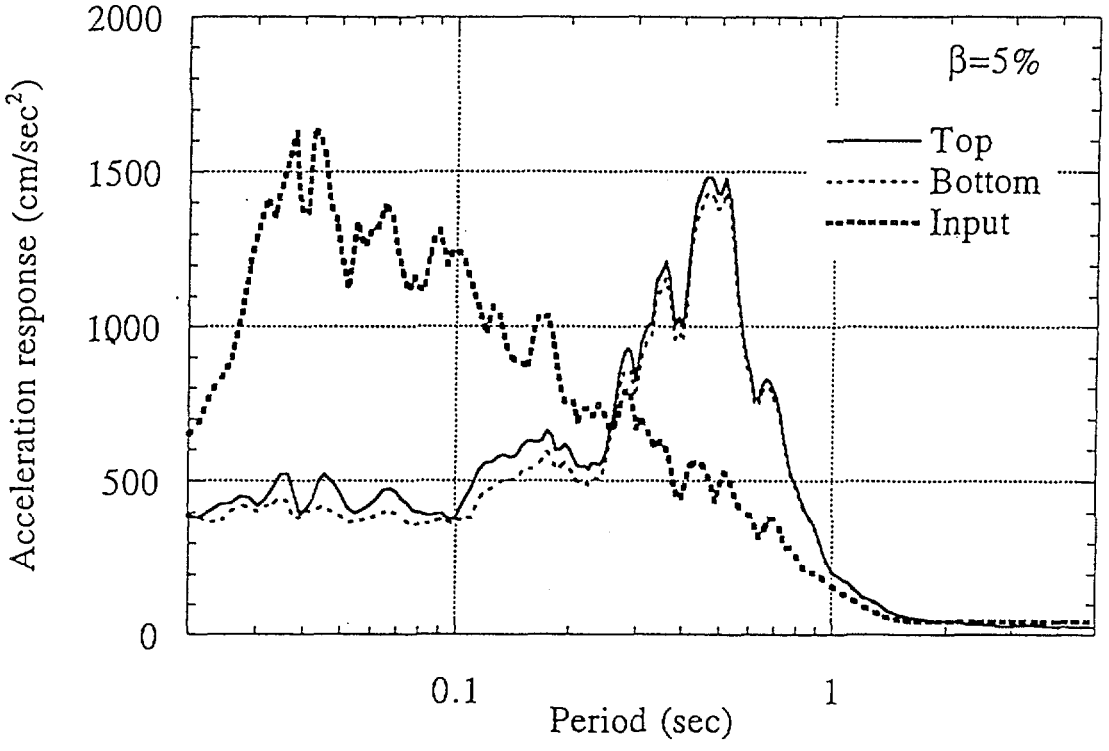

Fig. 25 Acceleration response spectra (test results, input: 1.5S1)

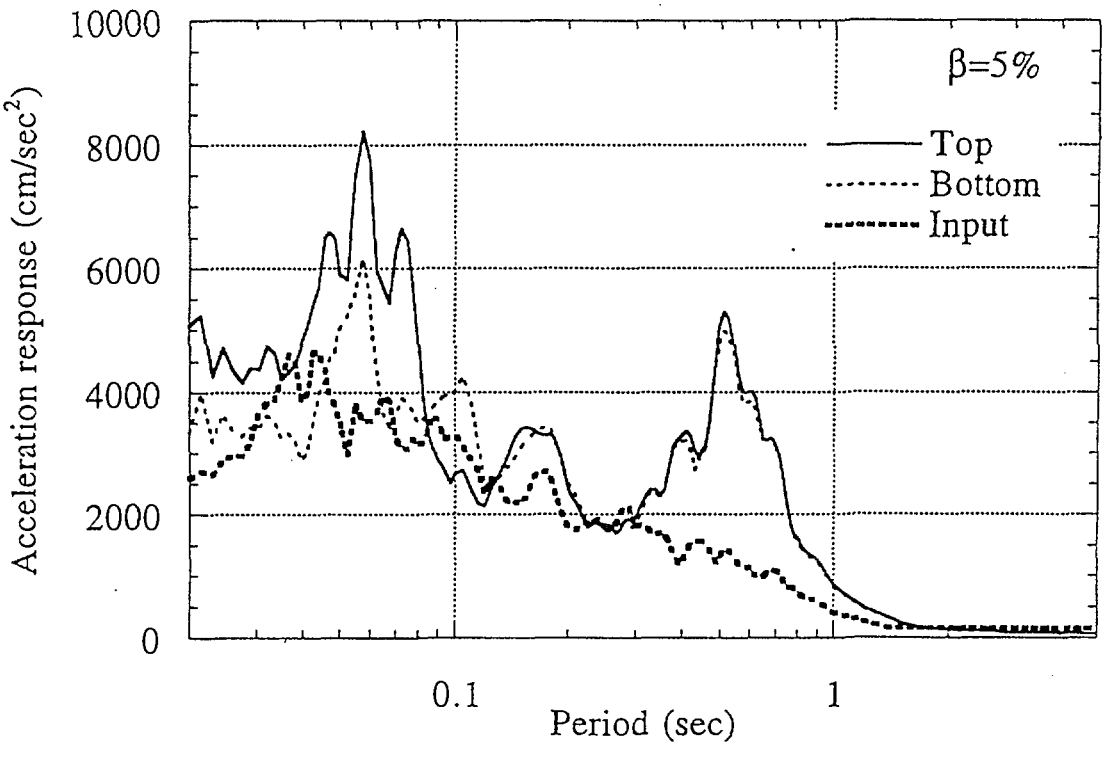

Fig. 26 Acceleration response spectra (test results, input: 4.6S1)

4.2. Test results

Figs. 22 through 24 show acceleration time histories of the shaking table, response accelerations at the top and the bottom of the rigid mass. Figs. 25 and 26 show acceleration response spectra with the damping 5% of critical at the top and the bottom of the rigid mass for the input earthquake motion of 1.5×S1 and 4.6×S1 (Measured acceleration amplitude of the shaking table in the test was 4.6 times as large as that of S1). In the case of the input earthquake motion of 1.5×S1, response spectra at the bottom and the top are similar and it is perceived that the rocking motion is small and the swaying motion is dominant. However, in the case of the input earthquake motion of 4.6×S1 difference of the spectra is perceived at the top and the bottom.

Figs. 27 and 28 show the force-displacement relationship of the rubber bearing during the shaking. In the case of the input earthquake motion of 1.5×S1 response shear deformation remains under the linear limit of the rubber bearing and hardening of the rubber bearing does not occur, whereas in the case of the input earthquake motion of 4.6×S1 the rubber bearing exceeds the linear limit and enters the hardening region causing the loss of isolation effect as shown in Fig. 26.

5. SIMULATION OF SHAKING TABLE TESTS

5.1. Simulation of CRIEPI shaking table test

5.1.1. Modeling of isolators

In the simulation, isolator was modeled in two ways. The first way is modeling isolator as a parallel combination of an elasto-plastic spring and an elastic spring (herein called bilinear model) as shown Fig. 29. In this case parameters of bilinear spring were determined from the static test result of HDR.

The second way is to model isolator as a parallel combination of several elasto-plastic springs and a non-linear elastic spring (herein called polylinear model) as shown in Fig. 29. Parameters specifying each elasto-plastic spring are determined so that the energy dissipated per one cycle becomes equal to that evaluated from the bearing test. Suppose stiffness and yield displacement of each elasto-plastic component are given as K_i and δ_i, and δ_i is corresponding to displacement amplitude of cyclic loading test of rubber bearing. Then energy dissipated per one cycle denoted by W_{i+1} at an amplitude of δ_{i+1} is given as

$$W_{i+1} = \sum_{l=0}^{i} 4(\delta_{i+1} - \delta_l)K_l\delta_l \quad (i = 0,1\cdots\cdots\cdots) \quad (7)$$

Subtracting W_i from W_{i+1} one can obtain

$$W_{i+1} - W_i = 4(\delta_{i+1} - \delta_i)\sum_{l=0}^{i-1} K_l\delta_l + 4(\delta_{i+1} - \delta_i)K_i\delta_i$$

$$= 4(\delta_{i+1} - \delta_i)\sum_{l=0}^{i-1}(Q_y)_l + 4(\delta_{i+1} - \delta_i)(Q_y)_i \quad (8)$$

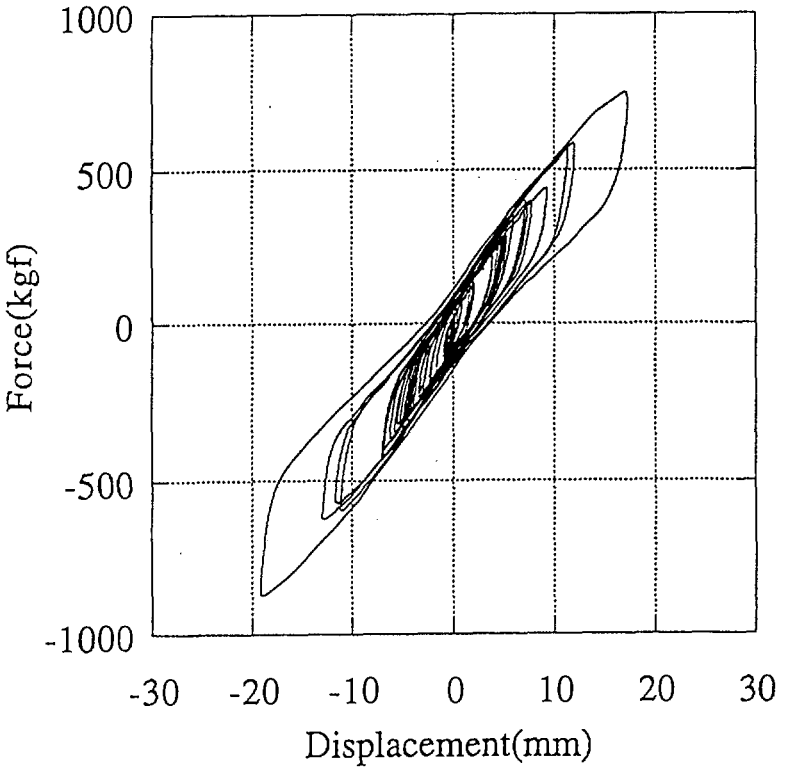

Fig. 27 Force -displacement relationship (test result, input: 1.5S1)

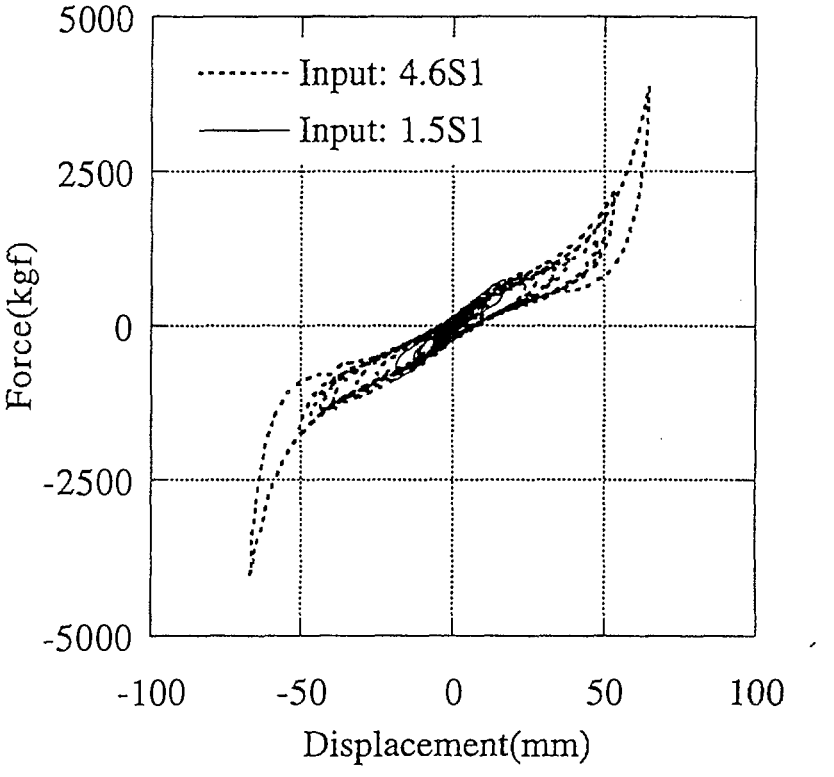

Fig. 28 Force -displacement relationship (test result, input: 4.6S1)

where $(Q_y)_i$ is the yielding force for i-th elasto-plastic spring, then each spring constant K_i of elasto-plastic spring is given as

$$K_i = \frac{(Q_y)_i}{\delta_i} = \frac{(W_{i+1} - W_i)}{4(\delta_{i+1} - \delta_i)} - \sum_{l=0}^{i-1} (Q_y)_l \times \frac{1}{\delta_i} \quad (9)$$

Eq. (9) is a recurrent formula, and $(Q_y)_i$, δ_i and W_i are given and evaluated from the experiment.

5.1.2. Simulation of base-isolated rigid mass

In the numerical simulation of the shaking table test, isolated structure is modeled as shown in Fig. 30. For the simulation of the test case where the response of the rubber bearing remains under the linear limit as shown in Fig. 27, simple bilinear spring is used to model the rubber bearing. Fig. 31 shows the comparison between the test result and the simulated result using bilinear model in terms of response spectrum for 1.5×S1 input motion. Both results agree fairly well. For this level of input motion bilinear modeling of the LRB gives enough accurate results. In these figures simulated results using polylinear model are shown as well. For the simulation where the response of the rubber bearing exceeds linear limit, several models are proposed which can take hardening effect, slip effect in the hysteresis of the rubber into account [10][17]. The polylinear model is one of those models. For the level of input motion 1.5×S1 simulated results using polylinear model show only slight difference compared with those using bilinear model.

5.2. Simulation of MISS shaking table test

The mock-up MISS is a Model of Isolated Steel Structure designed and manufactured in the research project conducted by ENEL/ENEA and the shaking table test was conducted at ISMES laboratory [3]. The model is a five-story steel frame and tested in different configurations, i.e. with/without additional masses and with/without base isolation. Base-isolated MISS is supported by 6 HDRs. In this CRP, the test data were provided by ENEL, and CRIEPI conducted numerical simulations of the tests for configuration C2 (16 masses base-fixed) and C3 (16 masses base-isolated) subjected to Tolmezzo NS earthquake component to short side direction (Y-direction) of the frame (test No. 135).

5.2.1. Eigen value analysis of base-fixed steel frame

At first, eigen value analysis for the base-fixed MISS (C2) was conducted. Eigen frequencies and modal participation factors are shown in Table 1. Mode shapes for principle modes are shown in Fig. 29. It is reported that the main frequencies in Y-direction evaluated from sine sweep test are 2.37Hz, 9.2Hz, 18.92Hz [3]. The result of the eigen value analysis shows good agreement with the experimental result.

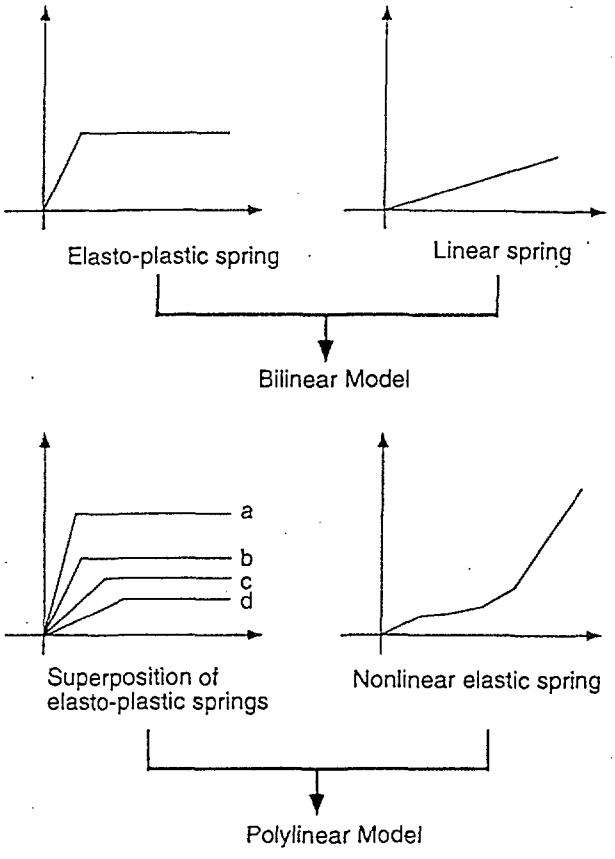

Fig. 29 Bilinear and polylinear model

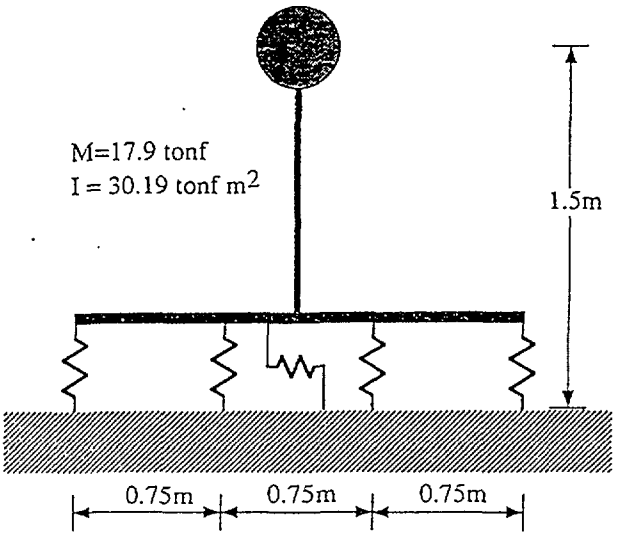

Fig. 30 Modeling of base-isolated rigid mass

Table 1 Eigen frequencies of base-fixed MISS

Order	Freq.(Hz)	Period(sec)	Modal participation factor (X)	Modal participation factor (Y)
1	2.60	0.39	1.04E-11	4.56E+00
2	3.77	0.27	-4.53E+00	7.25E-12
3	4.75	0.21	1.61E-11	1.86E-11
4	8.21	0.12	4.08E-13	1.48E+00
5	12.18	0.08	-1.54E+00	2.35E-13
6	14.69	0.07	-1.98E-12	7.63E-01
7	14.98	0.07	1.03E-12	5.09E-12
8	20.97	0.05	-2.30E-14	-3.49E-01
9	22.52	0.04	-8.30E-01	-1.71E-15
10	26.88	0.04	-4.89E-13	2.22E-13

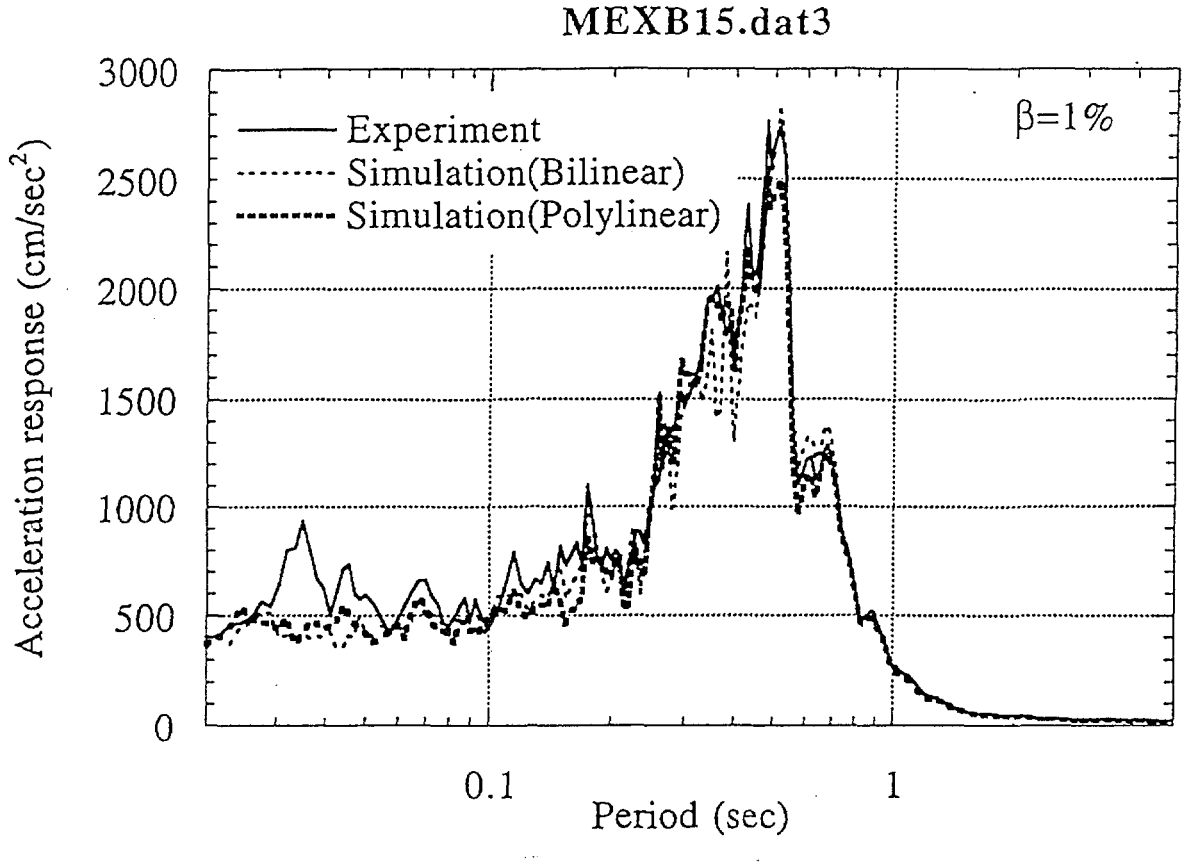

Fig. 31 Comparison of test and simulation for base-isolated rigid mass model (1.5S1 input)

5.2.2. Simulation of base-fixed steel frame

Using superstructure model used for eigen value analysis, response analysis was performed. Modal damping factor of 1.7% is given for the first mode, which was evaluated from the test, and for the rest of the modes modal damping factor of 0.85%(=1.7%/2) is given. Figs. 30 and 31 show acceleration time histories from the test and the simulation. Figs. 35 and 36 show FRS (Floor Response Spectra) obtained from the test and the simulation with damping of 1%. Agreement between both results can be perceived.

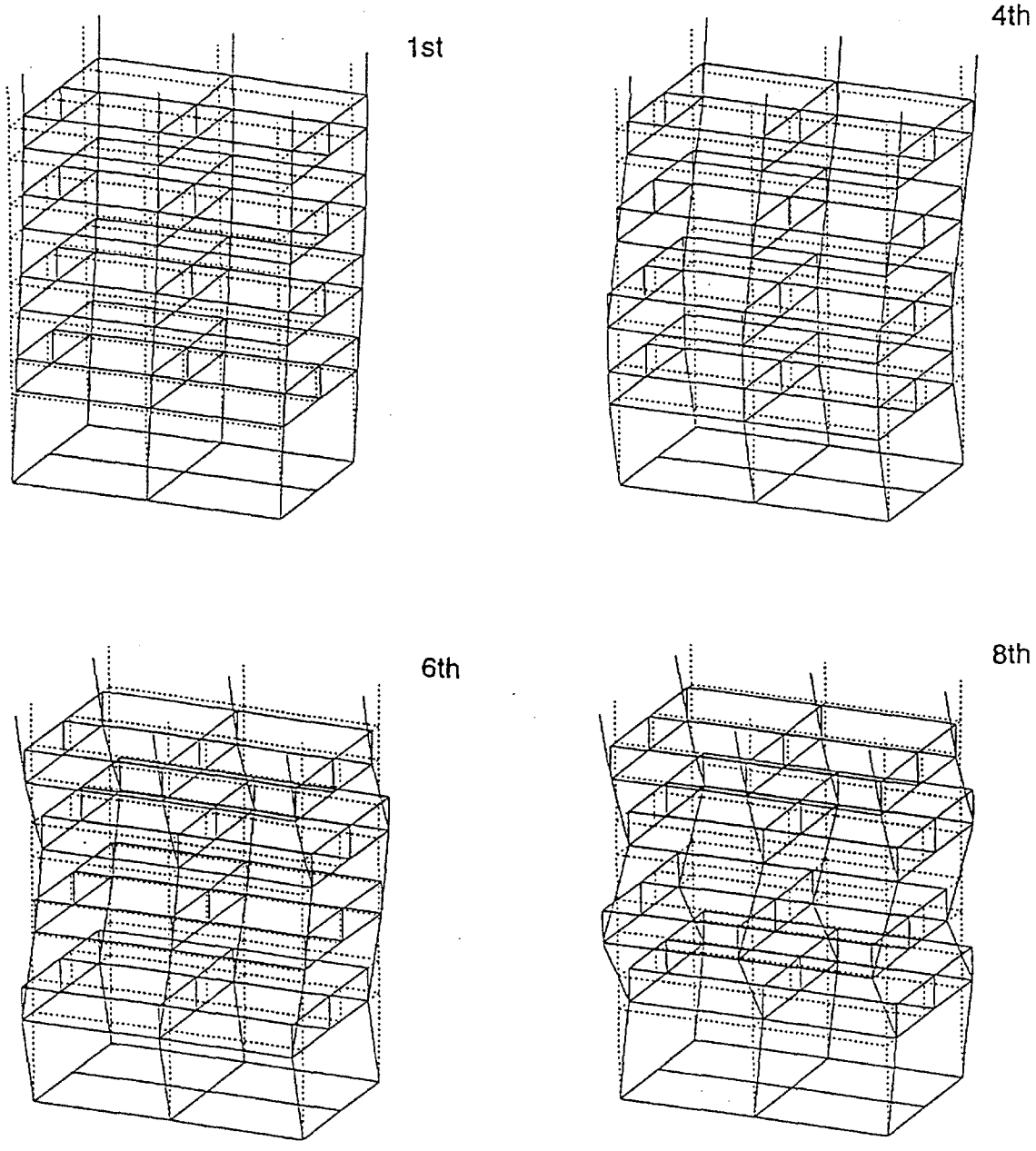

Fig. 32 Mode shape of base-fixed MISS

5.2.3. Simulation of base isolated steel frame

At first, exigent value analysis was conducted for base-isolated MISS, where HDR is modeled using bilinear model. Eigen frequencies and modal participation factors are shown in Table 2. Mode shapes for the principle modes are shown in Fig. 37. Modeling isolators in the way mentioned in *5.1.1*, response analyses of base-isolated MISS were performed. From the damping of the superstructure and the rubber bearing, weighted modal damping [15], which is proportional to the maximum strain energy, is evaluated. Weighted modal damping ratio is given by following equation.

$$\beta_{ieq} = \frac{\sum_j D_j k_j \Delta_{ij}^2 + D_{iso} k_{iso} \Delta I_{i-iso}^2}{\sum_j k_j \Delta_{ij}^2 + k_{iso} \Delta_{i-iso}^2} \quad (10)$$

where β_{ieq} is the modal damping ratio for i-th mode, D_j and D_{iso} are respectively damping ratio of the superstructure and the rubber bearing, k_j is stiffness of j-th member of the superstructure and k_{iso} is the total stiffness of the rubber bearings, Δ_{ij} is the i-th modal strain of j-th member of the superstructure and Δ_{i-iso} is the i-th modal displacement of rubber bearing. 1.7% of damping for the superstructure and 2% of additional damping for the rubber bearings are used.

HDRs used for the MISS are modeled by two models. One is bilinear model and the other is polylinear model. Parameters specifying these models are determined from the experimental results as described in *5.1.1*. Figs 38 and 39 show hysteresis loop of isolators in the numerical simulation compared with static rubber bearing test result. Comparisons of displacement response time history of rubber bearing are shown in Figs. 40 and 41, where bilinear model and polylinear model are used. Both simulation results show agreement with the test results to some extent, and in this case polylinear modeling did not necessarily give improvement. Fig. 42 shows comparison of the FRS obtained from the test and the simulation using bi-linear model for HDR. Around the fundamental period both results show agreement, however in shorter period range, discrepancy becomes larger. Fig. 43 shows the results of the simulation using polylinear model, and the improvement of the simulation is not perceived.

Text cont. on page 164.

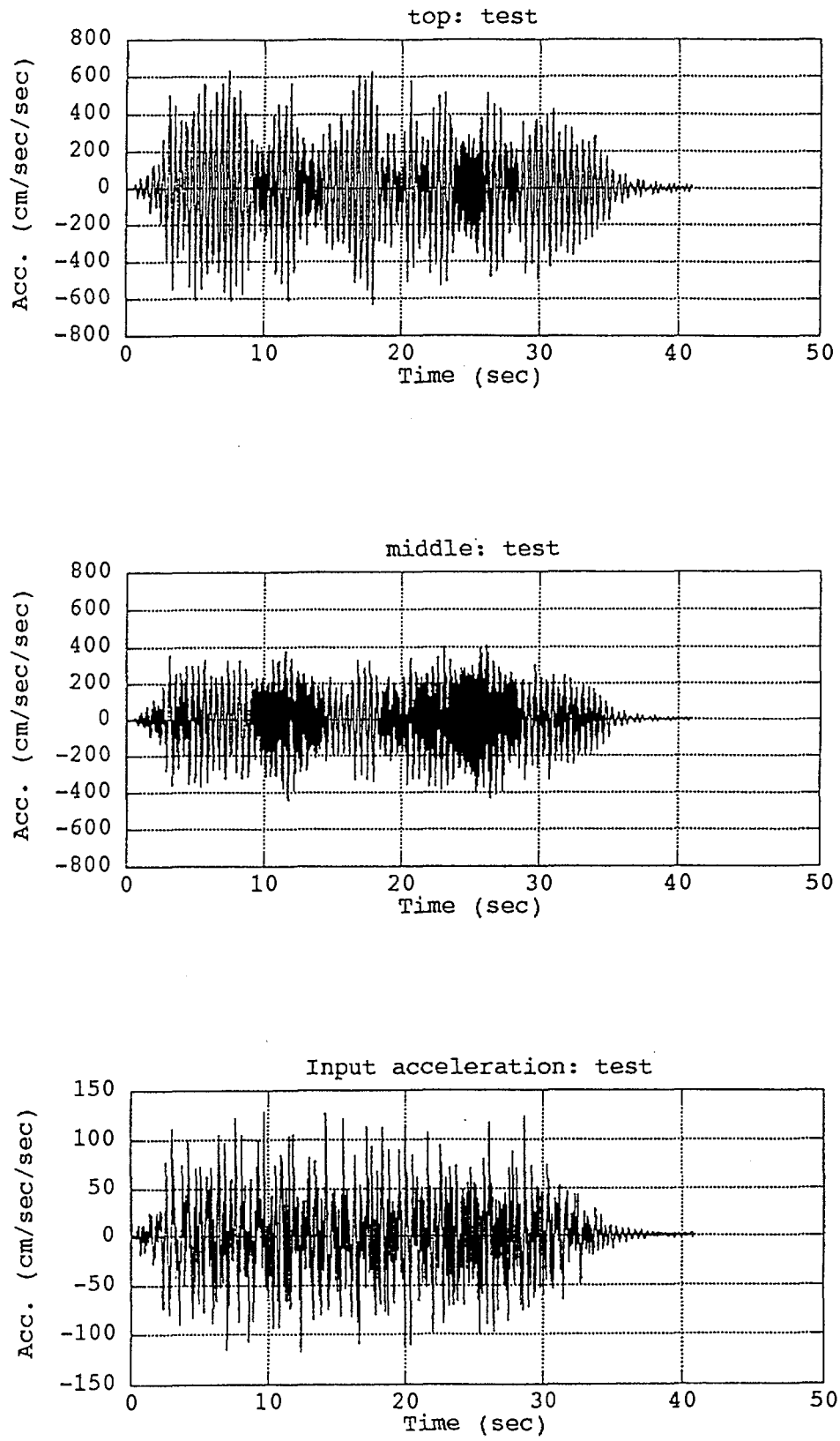

Fig. 33 Test results of acceleration response of base-fixed MISS (Tolmezzo NS)

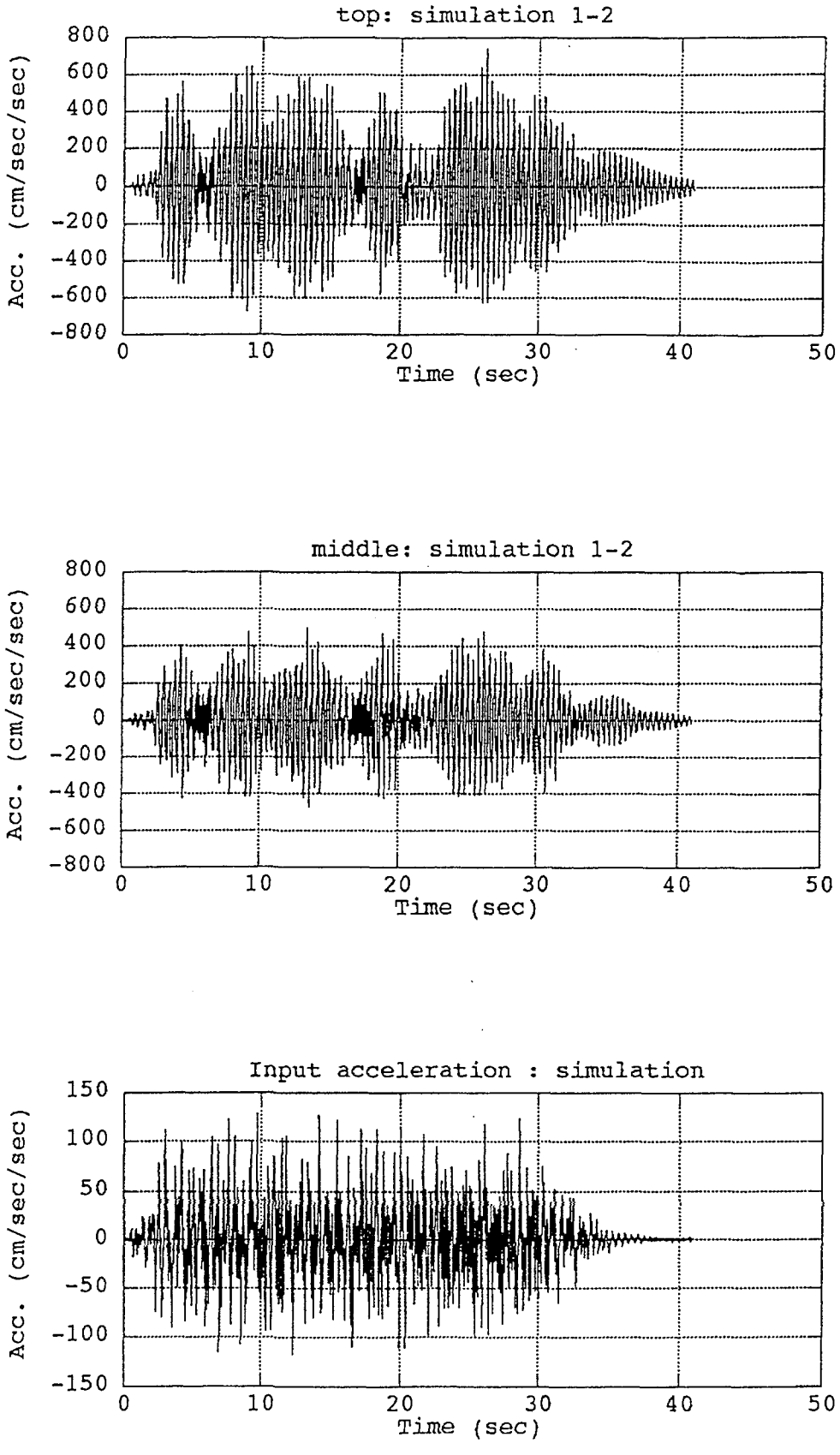

Fig. 34 Simulation results of acceleration response of base-fixed MISS (Tolmezzo NS)

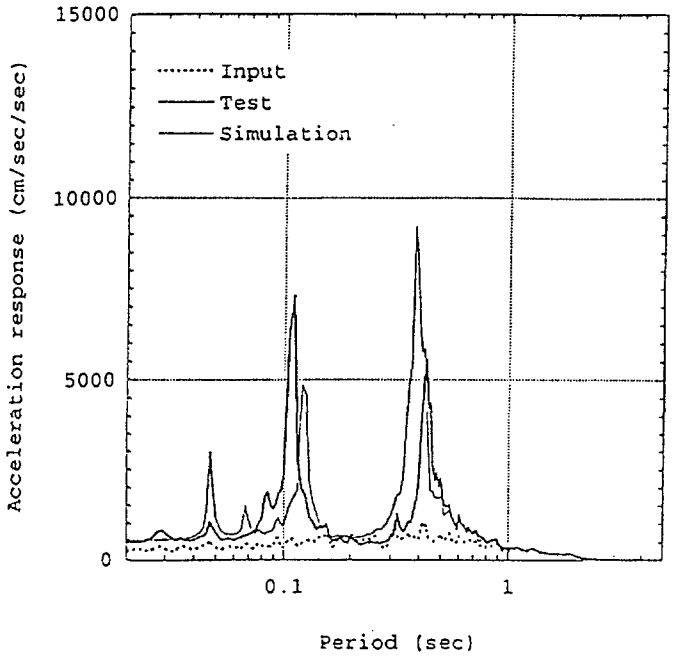

Fig. 35 Acceleration response spectra of base-fixed MISS (1% damping) test and simulation (at the middle level, model 3BH)

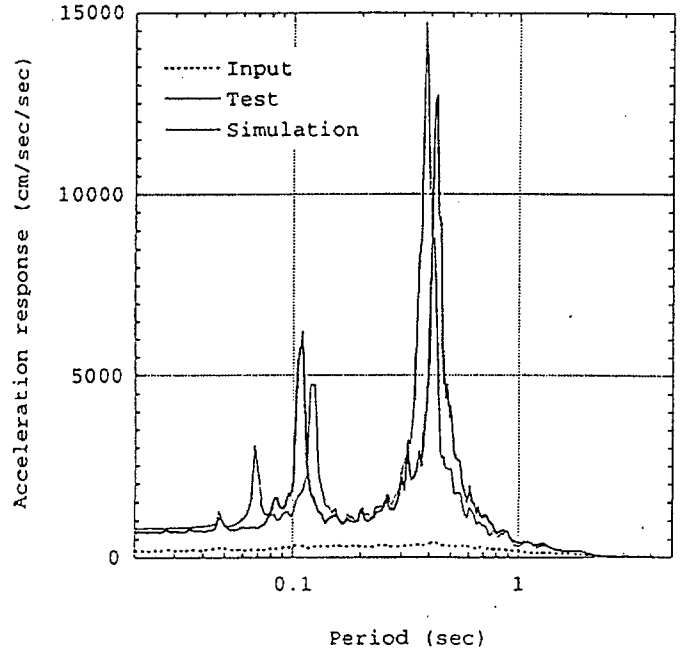

Fig. 36 Acceleration response spectra of base-fixed MISS (1% damping) test and simulation (at the top, model 3BH)

Table 2 Eigen frequencies of base-isolated MISS

Order	Freq.(Hz)	Period(sec)	Modal participation factor (X)	Modal participation factor (Y)
1	1.06	0.94	3.77E-10	5.01E+00
2	1.11	0.90	-5.01E+00	3.76E-10
3	4.55	0.22	5.31E-12	2.24E-11
4	5.69	0.18	1.52E-12	-2.96E-01
5	7.93	0.13	1.56E-01	5.33E-13
6	11.87	0.08	5.11E-14	8.04E-02
7	14.28	0.07	1.36E-12	-1.73E-12
8	17.41	0.06	-3.79E-02	8.35E-14
9	18.63	0.05	-2.68E-13	3.90E-02
10	23.72	0.04	-2.70E-14	-3.23E-02
11	25.60	0.04	4.33E-14	8.65E-14
12	28.49	0.04	1.67E-02	2.08E-14

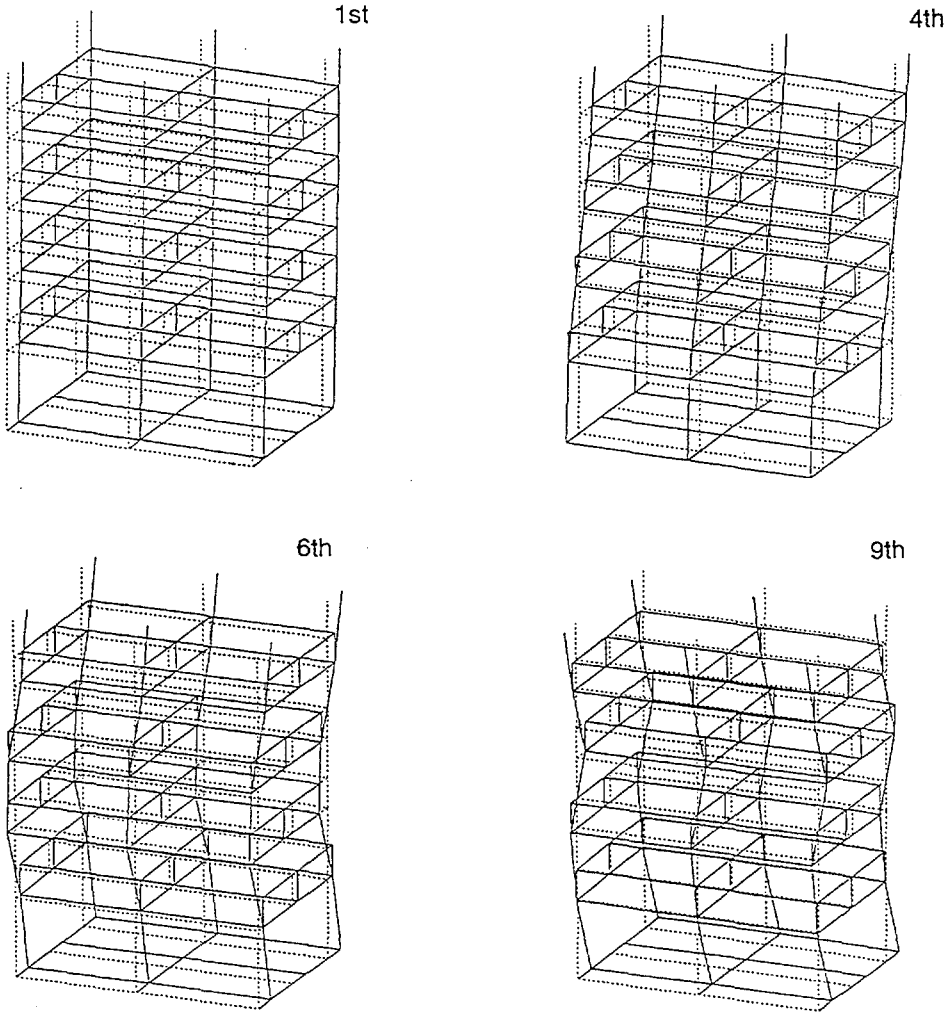

Fig. 37 Mode shape of base-isolated MISS

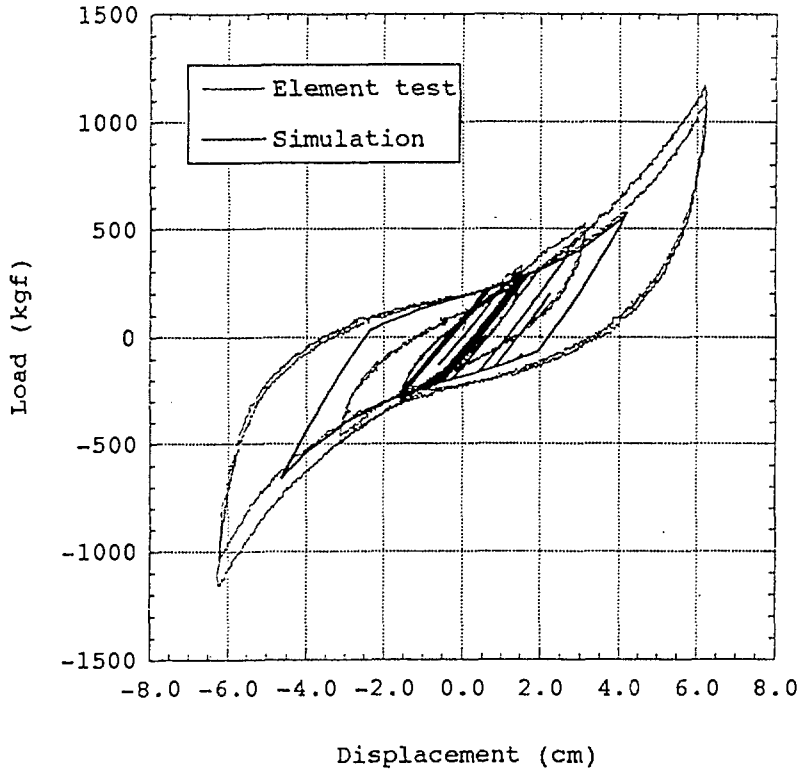

Fig. 38 Force -displacement relationship of HDR
(Simulation with bilinear model)

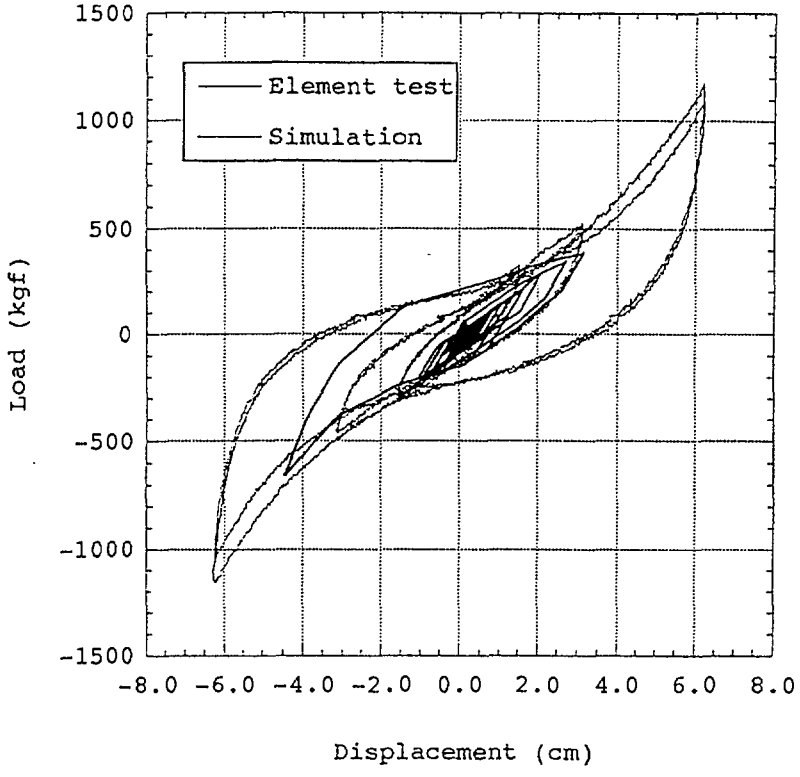

Fig. 39 Force -displacement relationship of HDR
(Simulation with polylinear model)

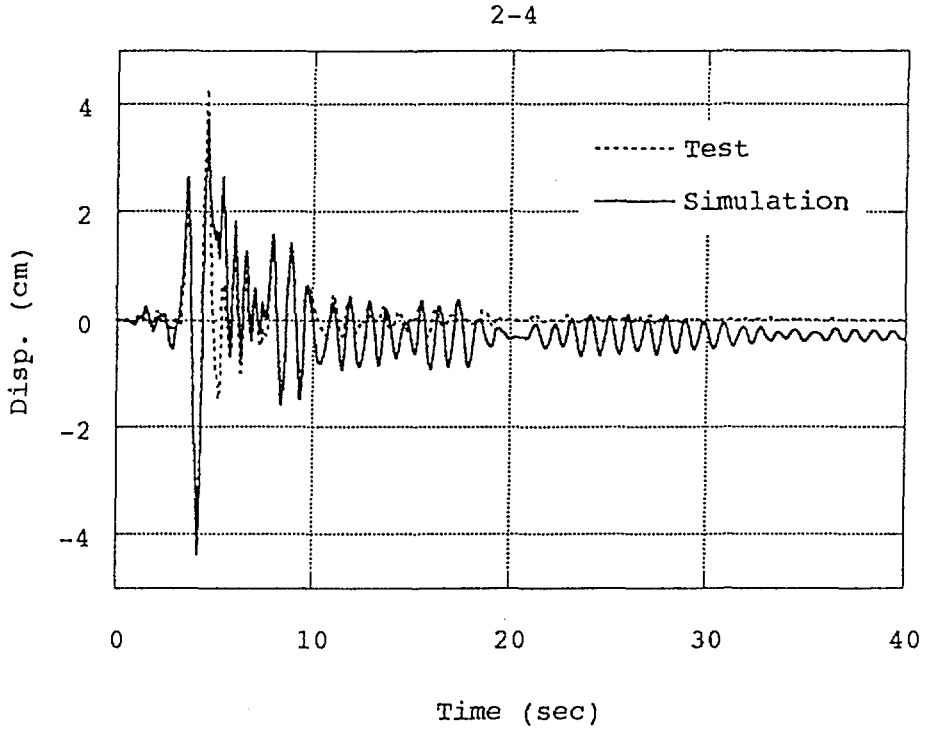

Fig. 40 Comparison of time displacement response of HDR (Simulation with bilinear model)

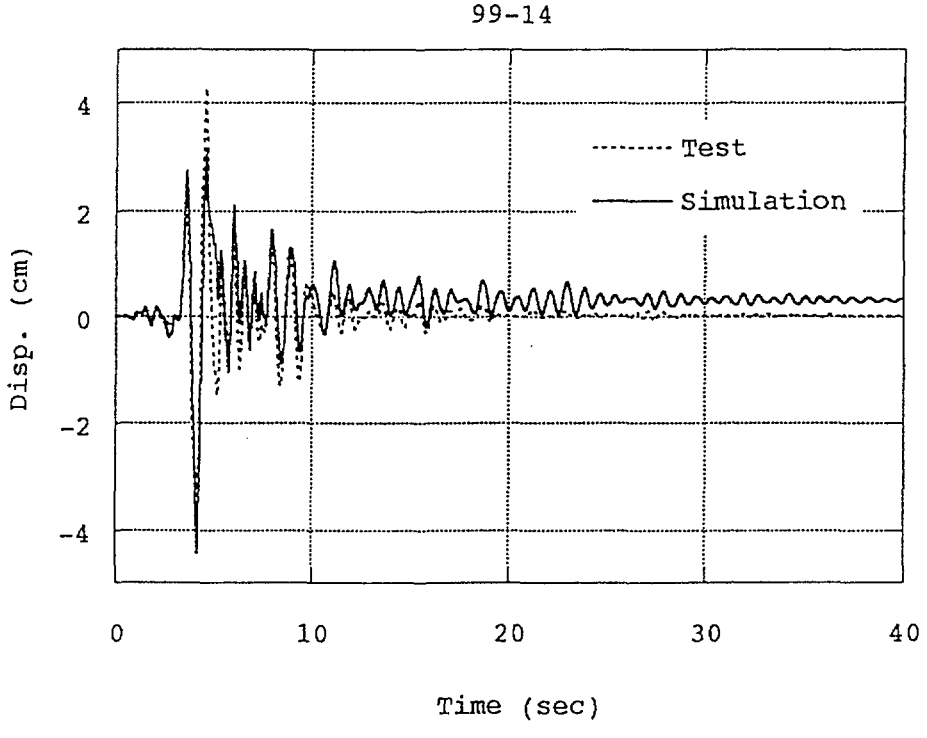

Fig. 41 Comparison of time displacement response of HDR (Simulation with polylinear model)

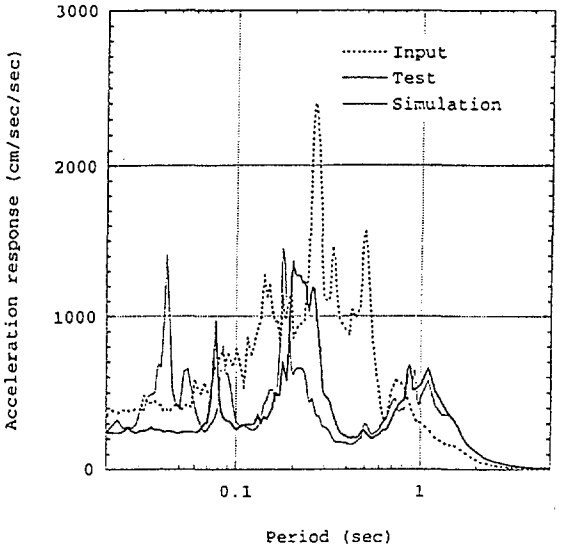

Acceleration response spectra (1% damping)
test and simulation (at the base)
(Base-isolated model, Tolmezzo NS)
sim. 2-4

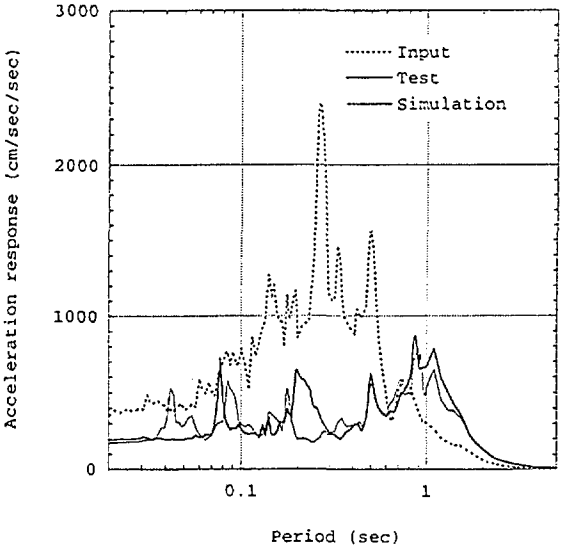

Acceleration response spectra (1% damping)
test and simulation (at the middle)
(Base-isolated model, Tolmezzo NS)
sim. 2-4

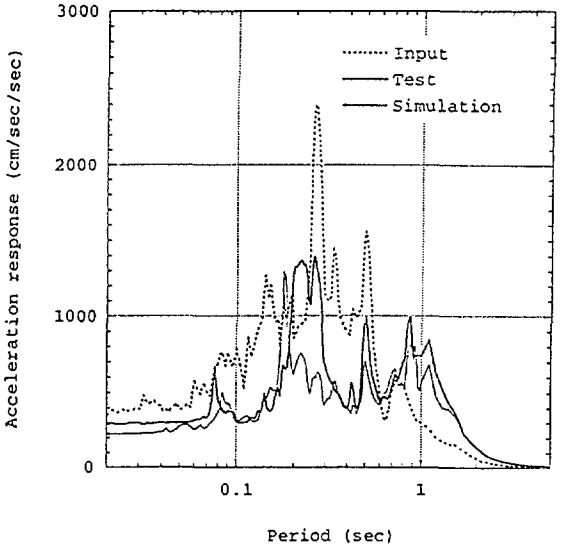

Acceleration response spectra (1% damping)
test and simulation (at the top)
(Base-isolated model, Tolmezzo NS)
sim. 2-4

Fig. 42 Comparison of FRS from test and simulation
(Simulation with bilinear model)

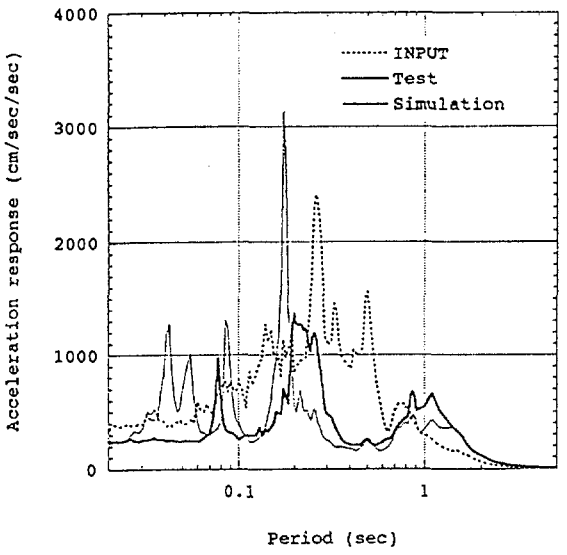

Acceleration response spectra (1% damping)
test and simulation (at the base)
(Base-isolated model, Tolmezzo NS)
sim. 99-14

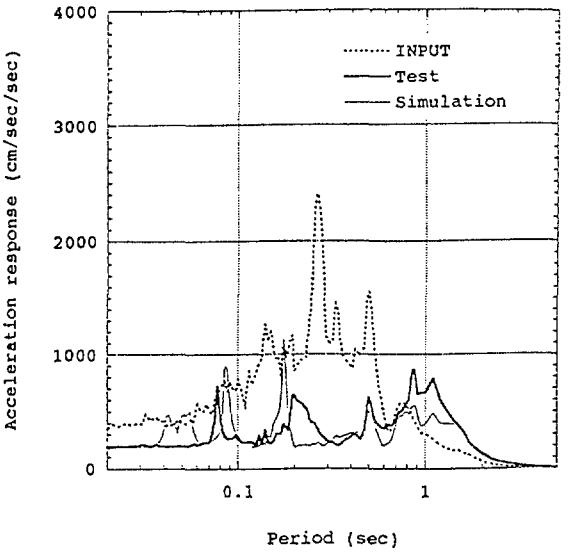

Acceleration response spectra (1% damping)
test and simulation (at the middle)
(Base-isolated model, Tolmezzo NS)
sim. 99-14

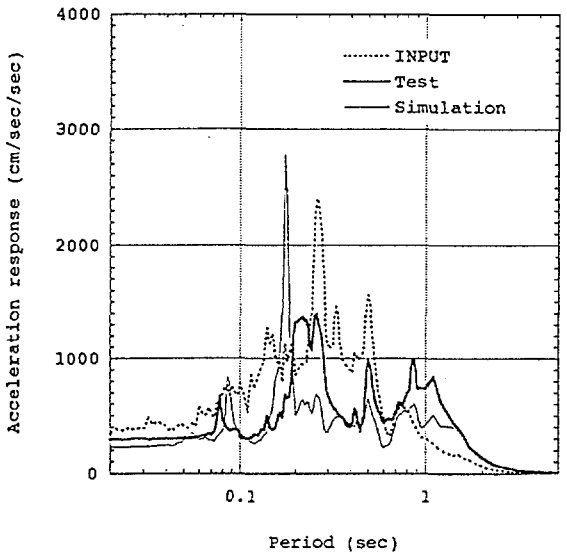

Acceleration response spectra (1% damping)
test and simulation (at the top)
(Base-isolated model, Tolmezzo NS)
sim. 99-14

Fig. 43 Comparison of FRS from test and simulation
(Simulation with polylinear model)

6. CONCLUSIONS

Using computer code ABAQUS, numerical simulations of rubber bearing tests are conducted for NRBs, LRBs (data provided by CRIEPI) and for HDRs (data provided by ENEA/ENEL and KAERI). Several strain energy functions are specified according to the rubber material test corresponding to each rubber bearing. As for lead plug material in LRB, mechanical characteristics are reevaluated and are made use of. Simulation results for these rubber bearings show satisfactory agreement with the test results.

Simulations of shaking table tests are conducted for this rigid mass model supported by LRBs and for the steel frame model supported by HDRs. In the simulation of the rigid mass model test, where LRBs are used, isolators are modeled either by bilinear model or polylinear model. In both cases of modeling of isolators, simulation results show good agreement with the test results. In the case of the steel frame model, where HDRs are used as isolators, bilinear model and polylinear model are also used for modeling isolators. The response of the model is simulated comparatively well in the low frequency range of the floor response; however, in the high frequency range discrepancies from the test result becomes larger, implying the requirement of more detailed or proper modeling of the rubber bearing and the steel frame.

ACKNOWLEDGEMENTS

Rubbers bearing tests and shaking table test carried out in CRIEPI were conducted in the research project "Verification Test of Seismic Isolation System for Fast Breeder Reactor" sponsored by Ministry of International Trade and Industry, Japan. LRB with thick lead plug was tested in the research project sponsored by Japan Atomic Energy Research Institute (JAERI) and Dr. Tada of JAERI is appreciated for providing the data. Authors would like to express their appreciation to Mr. S. Nomura of D.C.C. Ltd. for his contribution to the computational work.

REFERENCES

[1] Dusi, A and Bertola, S., et al., 1997, "Status of Italian activities on intercomparison of analysis methods for seismically isolated nuclear structures", International Post-SMiRT Conference Seminar on Seismic Isolation, Passive Energy Dissipation and Active Control of Seismic Vibration of Structures, Taormina, Italy

[2] Dusi, A., Forni, M. and Martelli, A., 1998, "Contribution of Italy to the activities on intercomparison of analysis methods for seismically isolated nuclear structures: Finite Element Analysis of lead rubber bearings", IAEA RCM material, Hertford, UK

[3] Forni, M., Martelli, A. and Dusi, A., 1998, "Contribution of Italy to the activities on intercomparison of analysis methods for seismically isolated nuclear structures: Shake table tests on a steel frame structure mock-up", IAEA RCM material, Hertford, UK

[4] Hirata, K., Matsuda, A. and Yabana, S., 1997, "Contribution of Japan to the activities on intercomparison of analysis methods for seismically isolated nuclear structures", Proc. International Post-SMiRT Conference Seminar on Seismic Isolation, Passive Energy Dissipation and Active Control of Seismic Vibrations of Structures, Taormina, Italy

[5] Hirata, K and Matsuda, A., 1999, "Contribution of Japan to the activities on intercomparison of analysis methods for seismically isolated nuclear structures", Proc. International Post-SMiRT Conference Seminar on Seismic Isolation, Passive Energy Dissipation and Active Control of Seismic Vibrations of Structures, Cheju, Korea

[6] Hibbitt, Karlson &Sorensen, Inc., 1996, "ABAQUS/Standard User's Manual"

[7] JSME, 1982, "Investigation report on the development of computer code for the structural analysis of spent fuel transport packaging (in Japanese)"

[8] Ishida, K., et al., 1991, "Failure tests of laminated rubber bearings", Trans. 11th SMiRT, vol. K2

[9] Ishida, K., Shiojiri, H, et al., 1992, "Shaking table test on ultimate behavior of seismic isolation system Part 2: Response behavior of rubber bearings", Proc. 10th WCEE, Barcelona, Spain

[10] Ishida, K., Yabana, S., et al., 1993, "Analytical study on ultimate response characteristics of base isolated structures", Trans. of 12th SMiRT, vol. K, Stuttgart, Germany

[11] Matsuda, A., Y. Otori, et al., 1999, "Simulation on the laminated rubber bearing tests using large deformation finite element method (in Japanese)", Trans. of JSME, vol. 65, No. 635 A

[12] Mazda, T., Moteki, M., et al., 1989, "Test on large-scale seismic isolation elements", Trans. 10th SMiRT, vol. K2

[13] Mazda, T., Shiojiri, H., et al., 1991, "Test on large-scale seismic isolation elements Part 2", Trans. 11th SMiRT, vol. K2

[14] Moteki, M, Kawai, N., et al., 1992, "Shaking table test on ultimate behavior of seismic isolation system Part 1: Outline of the test and response of superstructure", Proc. 10th WCEE, Barcelona, Spain

[15] Roesset, J.M, Whitman, et al., 1973, "Modal analysis for structures with foundation interaction", J. of St. Div., Proc. ASCE, ST3

[16] Seki, W., Fukahori, Y., et al., 1987, "A large-deformation finite-element analysis for multilayer elastomeric bearings", 133rd American Chemical Society, Rubber Division, Montreal, Canada

[17] Suhara, M., Takeda, M., et al, 1992, "Dynamic ultimate test of base-isolated system", Proc. 10th WCEE, Barcelona, Spain

[18] Yoo, B and Lee, J-H, 1997, "Intercomparison of analysis methods for seismically isolated nuclear structures (ENEA HDRB and CRIEPI LRB)", International Post-SMiRT Conference Seminar on Seismic Isolation, Passive Energy Dissipation and Active Control of Seismic Vibration of Structures, Taormina, Italy